# Neuroprotective effects of G9a inhibition through modulation of peroxisome-proliferator activator receptor gamma-dependent pathways by miR-128

Aina Bellver-Sanchis, Pedro A Ávila-López, Iva Tic, David Valle-García, Marta Ribalta-Vilella, Luis Labrador, Deb Ranjan Banerjee, Ana Guerrero, Gemma Casadesus, Coralie Poulard, et al.

NEURAL REGENERATION RESEARCH
www.nrronline.org

Research Article

# Neuroprotective effects of G9a inhibition through modulation of peroxisome-proliferator activator receptor gamma-dependent pathways by *miR-128*

**Aina Bellver-Sanchis[1], Pedro A. Ávila-López[2], Iva Tic[1], David Valle-García[3, †], Marta Ribalta-Vilella[1], Luis Labrador[4], Deb Ranjan Banerjee[5], Ana Guerrero[1], Gemma Casadesus[4], Coralie Poulard[6, 7, 8], Mercè Pallàs[1, 9], Christian Griñán-Ferré[1, 9, *]**

**https://doi.org/10.4103/1673-5374.393102**

**Date of submission: June 13, 2023**

**Date of decision: December 17, 2023**

**Date of acceptance: December 28, 2023**

**Date of web publication: January 8, 2024**

### *From the Contents*



### Graphical Abstract

***G9a inhibition modulates PPARγ-dependent pathways through miR-128, enhancing the mechanisms of oxidative stress, autophagy, apoptosis, DNA damage, and synaptic plasticity in Alzheimer's disease***

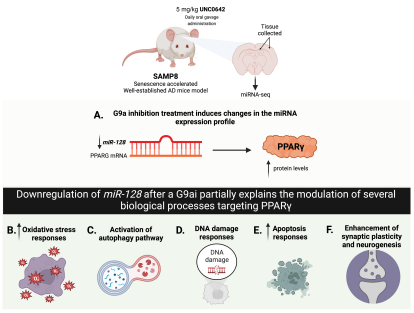


## Abstract

Dysregulation of G9a, a histone-lysine N-methyltransferase, has been observed in Alzheimer's disease and has been correlated with increased levels of chronic inflammation and oxidative stress. Likewise, microRNAs are involved in many biological processes and diseases playing a key role in pathogenesis, especially in multifactorial diseases such as Alzheimer's disease. Therefore, our aim has been to provide partial insights into the interconnection between G9a, microRNAs, oxidative stress, and neuroinflammation. To better understand the biology of G9a, we compared the global microRNA expression between senescence-accelerated mouse-prone 8 (SAMP8) control mice and SAMP8 treated with G9a inhibitor UNC0642. We found a downregulation of *miR-128* after a G9a inhibition treatment, which interestingly binds to the 3′ untranslated region (3′-UTR) of peroxisome-proliferator activator receptor γ (PPARG) mRNA. Accordingly, *Pparg* gene expression levels were higher in the SAMP8 group treated with G9a inhibitor than in the SAMP8 control group. We also observed modulation of oxidative stress responses might be mainly driven *Pparg* after G9a inhibitor. To confirm these antioxidant effects, we treated primary neuron cell cultures with hydrogen peroxide as an oxidative insult. In this setting, treatment with G9a inhibitor increases both cell survival and antioxidant enzymes. Moreover, up-regulation of PPARγ by G9a inhibitor could also increase the expression of genes involved in DNA damage responses and apoptosis. In addition, we also described that the PPARγ/AMPK axis partially explains the regulation of autophagy markers expression. Finally, PPARγ/GADD45α potentially contributes to enhancing synaptic plasticity and neurogenesis after G9a inhibition. Altogether, we propose that pharmacological inhibition of G9a leads to a neuroprotective effect that could be due, at least in part, by the modulation of PPARγ-dependent pathways by *miR-128*.

**Key Words:** aging; cognitive decline; epigenetics; G9a inhibition; microRNAs; miR-128; peroxisome-proliferator activator receptor γ (PPARγ); PPARG; SAMP8

[1]Department of Pharmacology and Therapeutic Chemistry, Institut de Neurociències-Universitat de Barcelona, Barcelona, Spain; [2]Department of Biochemistry and Molecular Genetics, Feinberg School of Medicine, Northwestern University, Chicago, IL, USA; [3]Institute of Biotechnology, National Autonomous University of Mexico, Cuernavaca, Mexico; [4]Department of Pharmacology and Therapeutics, Health Science Center-University of Florida, Gainesville, FL, USA; [5]Department of Chemistry, National Institute of Technology Durgapur, M G Avenue, Durgapur, West Bengal, India; [6]Cancer Research Cancer Lyon, Université de Lyon, Lyon, France; [7]Inserm U1052, Centre de Recherche en Cancérologie de Lyon, Lyon, France; [8]CNRS UMR5286, Centre de Recherche en Cancérlogie de Lyon, Lyon, France; [9]Centro de Investigación en Red, Enfermedades Neurodegenerativas (CIBERNED), Instituto de Salud Carlos III, Madrid, Spain
†Current address: Neuroimmunology Department, National Institute of Neurology and Neurosurgery "Manuel Velasco Suárez", Mexico City, Mexico
***Correspondence to:** Christian Griñán-Ferré, PhD, Christian.grinan@ub.edu.
https://orcid.org/0000-0002-5424-9130 (Christian Griñán-Ferré)

***Funding:*** *This study was supported by the Ministerio de Economía, Industria y Competitividad (Agencia Estatal de Investigación, AEI; to CGF and MP) and Fondo Europeo de Desarrollo Regional (MINECO-FEDER) (PID2022-139016OA-I00, PDC2022-133441-I00; to CGF and MP), Generalitat de Catalunya (2021 SGR 00357; to CGF and MP). This study was co-financed by Secretaria d'Universitats i Recerca del Departament d'Empresai Coneixement de la Generalitat de Catalunya 2021 (Llavor 00086; to CGF). AG is the recipient of an Alzheimer's Association Research Fellowship (AARF-21-848511). ABS acknowledges the Agència de Gestió d'Ajuts Universitaris i de Recerca (AGAUR) for her FI-SDUR fellowship (2021FISDU 00182).*

***How to cite this article:*** *Bellver-Sanchis A, Ávila-López PA, Tic I, Valle-García D, Ribalta-Vilella M, Labrador L, Banerjee DR, Guerrero A, Casadesus G, Poulard C, Pallàs M, Griñán-Ferré C (2024) Neuroprotective effects of G9a inhibition through modulation of peroxisome-proliferator activator receptor gamma-dependent pathways by miR-128. Neural Regen Res 19(11):2532-2542.*

## Introduction

Dysregulation of epigenetic mechanisms has been widely implicated in various disease states with emphasis on neurodegenerative disorders (Griñán-Ferré et al., 2018). Alzheimer's disease (AD) is a progressive and debilitating neurological disorder characterized by a gradual and permanent decline in intellectual functioning and the ability to carry out daily activities. A complex combination of genetic, environmental, and lifestyle factors has been described as a potential cause of AD (Eid et al., 2019). With aging there are epigenetic alterations that promote dramatic changes in gene pattern profiles related to cognition, learning and memory formation, being relevant for the progression of age-related cognitive decline exhibited in AD pathology (Harman and Martín, 2020). Interestingly, global histone changes related to transcriptional activation and repression have been observed in different regions of postmortem AD brains (Park et al., 2022). Indeed, during aging and senescence, epigenetic alterations are detected, such as DNA methylation (5-mC) and hydroxymethylation changes (5-hmC), and several important chromatin modifications such as H3K4me, H3K9me, H3K27me, H4K16ac, among others (Tecalco-Cruz et al., 2020).

Noteworthily, the expression of non-coding RNA transcripts, including microRNAs (miRNAs) is altered at the epigenetic level in several age-related diseases such as AD (Cosín-Tomás et al., 2018). miRNAs are small noncoding RNAs, comprised of ~22 nucleotides, that negatively regulate gene expression via either degrading the target mRNA or by direct translational inhibition (Ha and Kim, 2014). Regarding AD progression, miRNAs have been identified as one of the crucial players in the constellation of physiological changes presented in AD patients (Cosín-Tomás et al., 2018; Wei et al., 2020). Interestingly, altered miRNA expression has been widely documented in AD and other neurodegenerative diseases, and several studies have linked these to neuroinflammation (Liang and Wang, 2021), oxidative stress (OS; Konovalova et al., 2019), and synaptic dysfunction (Siedlecki-Wullich et al., 2019) among others. Treatment of neuronal cells with histone deacetylase inhibitors, DNA methyltransferase inhibitors (DNMTi), or G9a inhibitors (G9ai) has shown to change miRNA expression pattern profile (Nagaraj et al., 2019; Shukla and Tekwani., 2020).

Epigenetic regulation by the methyltransferase G9a (also called EHMT2, the euchromatic histone methyltransferase 2) acts as a crucial regulator in human diseases and is particularly involved in learning and memory formation (Gupta-Agarwal et al., 2012). G9a mediates the H3K9me2 epigenetic mark, which is mainly associated with transcriptional repression (Shankar et al., 2013). Of note, G9a overexpression in the brain of late-stage familial AD mice (5×FAD) and AD patients has recently been demonstrated (Griñán-Ferré et al., 2019; Zheng et al., 2019). Our group previously demonstrated that pharmacological inhibition of G9a by UNC0642 produced significant neuroprotective effects in an early-onset AD mouse model (Griñán-Ferré et al., 2019; Bellver-Sanchis et al., 2023). On the one hand, we found an uncharacterized mechanism through glia maturation factor beta by which G9a inhibition promotes the reduction of neuroinflammation and increases synaptic plasticity through modifying the transcriptome of senescence-accelerated mouse-prone 8 (SAMP8) mice (Bellver-Sanchis et al., 2023). Moreover, it has been shown that G9a potentiates oxidative stress in neurons, and that its inhibition reduces reactive oxygen species levels and elevates antioxidant enzyme levels (Griñán-Ferré et al., 2019). Additionally, it is noteworthy that hydrogen peroxide ($H_2O_2$) treatment in cell cultures was shown to be associated with a pronounced increase in the repressive mark H3K9me2 (Rothammer et al., 2022). Then, G9a plays an important role in regulating gene expression with a neuroprotective effect.

Besides epigenetic marks, neuroinflammation (Leng and Edison, 2021) and OS (Ionescu-Tucker and Cotman, 2021) have a great impact on AD. Interestingly, *miR-128* knockout inhibits the progression of AD pathology in mouse models as a consequence of increased peroxisome proliferator-activated receptor gamma (PPARγ) levels (Liu et al., 2019). PPARγ is a ligand-activated transcription factor of the nuclear hormone receptor superfamily, which regulates several essential genes in various metabolic processes and cell fate, and it is also implicated in homeostasis and inflammation (Houseknecht et al., 2002). Of note, PPARγ is implicated in the OS response, inflammation, and apoptosis after brain injury or neurodegenerative disease (Kapadia et al., 2008; Yonutas and Sullivan, 2013). Previous reports demonstrated that PPARγ expression is positively upregulated by several transcription factors such as C/EBP, Krox20, and KLF4, among others (Liu et al., 2006; Cho et al., 2009; Wang et al., 2010; Ge et al., 2016). At the epigenetic level, *Pparg* gene expression is upregulated by H3K4me3. Furthermore, one study traced the repression of *Pparg* gene expression through the G9a-dependent addition of H3K9me2 to the entire *Pparg* gene body (Wang et al., 2013).

SAMP8 is a well-established mouse model to study age-related cognitive decline and AD hallmarks (Butterfield and Poon, 2005; Liu et al., 2020). Thus, the SAMP8 mouse is an interesting tool to unveil epigenetic alterations associated with AD (Griñán-Ferré et al., 2018). Furthermore, some recent studies have confirmed the relevance of epigenetic alterations in the onset and progression of the neurodegenerative process in the SAMP8 mice (Griñán-Ferré et al., 2018; Harman and Martín, 2020; Tecalco-Cruz et al., 2020).

Focusing on individual components of AD pathogenesis, in this study, we aim to explore how G9a, miRNAs, OS, and neuroinflammation are interconnected. Of note, the regulation of miRNA expression by G9a in AD remains elusive. Here, we hypothesize that G9a inhibition promotes changes in miRNA expression profiles in the SAMP8 mice, consequently modulating distinct events relevant to AD and ultimately promoting neuroprotective effects. We explored differentially expressed mRNA and miRNAs after G9a inhibition to find new molecular pathways and targets. Furthermore, using Gene Ontology (GO) database (http://geneontology.org/) and Kyoto Encyclopaedia of Genes and Genomes (KEGG) database (https://www.kegg.jp/) pathway analyses, we unveil a novel mechanism by which G9a inhibition promotes beneficial effects on cognition in the SAMP8 mouse (see results related to cognitive status after G9ai treatment in (Bellver-Sanchis et al., 2023).

## Methods

### Animals

Female and male SAMP8 24-week-old mice (*n* = 20; Envigo, Sant Feliu de Codines, Barcelona, Spain, RRID: MGI:2160863) were used to perform cognitive and molecular studies. The mice were randomly allocated into two groups: SAMP8 control (*n* = 10), and SAMP8 treated with UNC0642 G9a inhibitor (SAMP8 UNC0642 (5 mg/kg); *n* = 10). The sample size for the intervention was chosen following previous studies (Bellver-Sanchis et al., 2023) in our laboratory and using one interactive tool (http://www.biomath.info/power/index.html). Experimental groups received a daily dose of either vehicle (2% w/v, (2-hydroxypropyl)-β-cyclodextrin) or a dose of 5 mg/kg per day of UNC0642 (BLDpharm, Shangai, China, #BD630326) dissolved in 2% 2-hydroxypropyl-β-cyclodextrin (Atomole Scientific Co. Ltd., Wuhan, Hubei, China, #AT-20762) via oral gavage for 4 weeks (Griñán-Ferré et al., 2019; Bellver-Sanchis et al., 2023). Animals had free access to food and water and were kept under standard temperature conditions (22 ± 2°C) and a 12-hour light-dark cycle (300 lx/0 lx).

All studies and procedures for the mouse behavior tests, brain dissection, and extractions followed the ARRIVE standard ethical guidelines (European Communities Council Directive 2010/63/EU and Guidelines for the Care and Use of Mammals in Neuroscience and Behavioral Research, National Research Council 2003) and were approved by the Institutional Animal Care and Generalitat de Catalunya (#222/18). All efforts were made to minimize the number of mice used and their suffering.

APP/PS1 mice were used as a source of primary cell cultures for *in vitro* experiments. Animals were socially caged (2–4 mice per cage) and maintained on a 12-hour light-dark cycle (lights on at 08:00 and off at 20:00) in a temperature-controlled room (22 ± 2°C). Food and water were available *ad libitum*. The use of these animals for primary culture was approved of under UF IACUC protocol 202011245. The protocol including the collection of fetal tissue was approved 1/19/2021.

### Biochemical experiments

#### *Brain processing*

An intraperitoneal injection of 10 mg/kg of ketamine (Imalgene 500, Rhone-Merieux) and 1 mg/kg of xylazine (Rompun, Bayer) diluted in NaCl 0.9% was used to euthanize SAMP8 mice 3 days after starting behavioral tests (see results of the behavioral tests in Bellver-Sanchis et al., 2023). Brains were immediately removed from the skull. The cortex and hippocampus were quickly isolated and frozen on powdered dry ice. They were maintained at –80°C for biochemical experiments. All reagents and kits used for the protocols described below are listed in **Additional Table 1**.

#### *miRNA sequencing*

Pools of four cortex tissue samples from the SAMP8 control and SAMP8 UNC0642 mice were used. To determine the altered miRNAs after treatment with UNC0642 we used the QIAseqmiRNA platform. TMM normalization and differential expression analysis were carried out using the edgeR program (Wang et al., 2013). The cutoff of differential miRNA was a fold-change threshold of 1.9 and a *P*-value < 0.05. The miRTarVis tool was used to predict miRNA targets (Jung et al., 2015).

Volcano plot, KEGG, Gene Ontology, and GSEA were used to perform the enrichment and pathway analysis (Subramanian et al., 2005) by using the Enrichr database (http://amp.pharm.mssm.edu/Enrichr; Chen et al., 2013; Kuleshov et al., 2016; Xie et al., 2021), and considering a *P*-value < 0.05 as statistically significant. Raw data were deposited at the Gene Expression Omnibus for miRNA-seq on mouse hippocampus SAMP8 (accession GSE189248).

#### *miRNA extraction and quantitative reverse transcription-polymerase chain reaction (qRT-PCR)*

miRNA was isolated from 100-125 mg of cortex tissue using the mirVana™ miRNA Isolation kit (Applied Biosystems, Foster City, CA, USA, #AM1560) (*n* = 6 per experimental group). Reverse transcription from RNA to first-strand complementary DNA (cDNA) was obtained using the TaqMan miRNA Reverse Transcription kit (Thermo Fischer Scientific, Waltham, MA, USA, #4366596) following manufacturer indications. Afterwards, amplification was performed from 1.33 µL of cDNA mixed with TaqMan™ Universal PCR Master Mix (Applied Biosystems, Vilnius, Lithuania, #4369016), and 20× RT primer (**Additional Table 2**) using the Step One Plus Detection System (Applied Biosystems, #4376600). Data were analyzed utilizing the ΔΔCt method, where the reference gene for miRNA (*U6 snRNA*) level was used to normalize differences in sample loading and preparation.

#### *RNA extraction and gene expression determination*

Total RNA isolation from cortical samples (*n* = 6 per experimental group) was carried out using TRItidy G™ reagent (PannReac AppliChem, Castellar del Vallès, Barcelona, Spain, #A4051, 0,200) following the manufacturer's instructions. The yield, purity, and quality of the RNA were determined spectrophotometrically with a NanoDrop™ ND-1000 apparatus (Thermo Fisher Scientific, Waltham, MA, USA) and an Agilent 2100B Bioanalyzer (Agilent Technologies, Santa Clara, CA, USA). RNAs with 260/280 ratios and RIN higher than 7.5, respectively, were selected. Reverse transcription-polymerase chain reaction (RT-PCR) was performed using the high-capacity cDNA Reverse Transcription kit (Applied-Biosystems, Vilnius, Lithuania, #4368813). SYBR® Green real-time PCR (Applied-Biosystems, #K0253) was performed to quantify the mRNA expression of a set of genes listed in **Additional Table 3** on a Step One Plus Detection System (Applied-Biosystems, #4376600). Data were analyzed utilizing the comparative cycle threshold (Ct) method (ΔΔCt), where the housekeeping gene level was used to normalize differences in sample loading and preparation. Normalization of expression levels was performed with β-actin for SYBR® Green-based real-time PCR results. Each sample was analyzed in triplicate, and the results represented the n-fold difference of the transcript levels among different groups.

***Western blotting***

Protein extracts were obtained from the hippocampal brain tissue samples taken after behavioral tests (see results of the behavioral tests in (Bellver-Sanchis et al., 2023). Tissues were homogenized in a cold RIPA lysis buffer (Sigma-Aldrich, Saint Louis, MO, USA, #R0278-50ML) supplemented with protease and phosphatase inhibitors, ultrasonicated, and centrifuged ($n$ = 6 mice per group). Firstly, the protein concentration of the supernatants was determined using the Bradford protein assay (Bio-Rad, Hercules, CA, USA, #5000006) while later proteins were separated by SDS-PAGE (12–14%) at 120 V and transferred to PVDF membranes by electroblotting at 200 mA for 120 minutes. Afterward, membranes were blocked in 5% BSA in 0.1% Tween20-TBS (TBS-T) for 1 hour at room temperature (RT), followed by overnight incubation at 4°C with the primary antibodies presented in **Additional Table 4**. By enhancing a chemiluminescence-based detection kit (Millipore, Burlington, MA, USA, #WBKLS0500) and Amersham Imager 680 (GE Healthcare, Chicago, IL, USA), we visualized immunoreactive proteins on digital images. Semi-quantitative analyses were carried out using ImageLab Software (BioRad, Hercules, CA, USA, SCR_014210) and results were expressed in Arbitrary Units (AU), considering the control mice group as 100%. Protein loading was routinely monitored and normalized by immunodetection of glyceraldehyde 3-phosphate dehydrogenase (GAPDH). Antibodies are listed in **Additional Table 4**.

***Cell culture***

Primary hippocampal neuron cultures were obtained from APP/PS1 mice brains on embryonic day 17. After dissection, the hippocampus was dissociated from the brain and digested with 0.25% trypsin (Gibco, Waltham, MA USA, #25200056). Digestion was stopped by adding DMEM-F12 medium (Gibco, #12400-024) with 10% fetal bovine serum (FBS) (Cytiva, Marlborough, MA, USA, #SH30088.03), after which the tissue was dispersed. The cells were resuspended in DMEM-F12 medium with 10% FBS and plated in poly-D-lysine (Santa Cruz Biotechnology, Dallas, TX, USA, #sc-136156) coated culture dishes at a density of 4–5 × $10^5$ cells/well. After 3 hours, the medium was replaced with serum-free Neurobasal medium (Gibco, #21103049) supplemented with B27 supplement (Gibco, #17504044), GlutaMAX™ (Gibco, #35050061), and 100× penicillin-streptomycin (P/S) (Gibco, #15140-122). Half of the medium was replaced every 2 days with fresh medium for 14 days allowing differentiation.

***Cytotoxicity test***

First, the cells were pretreated with a G9a inhibitor or vehicle. After 30 minutes, $H_2O_2$ was added to some wells at 500 µM. Cell viability was measured 24 hours after both treatments. The cytotoxicity of $H_2O_2$ was evaluated by the LDH assay (Roche, Indianapolis, IN, USA, #4744926001). Briefly, cell media was collected after each treatment and the collected media was mixed with LDH substrate in a 96-well plate. After incubation for 30 minutes at room temperature, the optical density was measured at 490 nm using a microplate reader (Molecular Devices, Sunnyvale, CA, USA). The measured optical density was then converted after standardization with negative (4% Triton X-100 (Sigma-Aldrich, #9036-19-5; 0% survival) and positive controls (1% Triton X-100; 100% survival).

***Data analysis***

Data analysis was performed using GraphPad Prism ver.9.2 software (GraphPad Software, San Diego, CA, USA, www.graphpad.com). Data were expressed as the mean ± standard error of the mean (SEM) from at minimum eight samples per group for behavioral tests (see results of the behavioral tests in Bellver-Sanchis et al., 2023) and four samples for molecular techniques. Means were compared with one-way analysis of variance followed by Tukey's *post hoc* analysis. Comparison between groups was also performed by two-tail Student's *t*-test for independent samples. Statistical significance was considered when *P*-values were < 0.05.

## Results

### G9a inhibition treatment induces changes in the miRNA expression profile

Alterations in miRNAs have been associated with aging and cognitive decline (Cosín-Tomás et al., 2018). Moreover, specific miRNA abnormal levels have been detected in several areas of the AD brain (Wang et al., 2019). Thus, to gain insight into the biology of G9a inhibition treatment, we analyzed the global miRNA expression between SAMP8 control and SAMP8 treated mice with UNC0642 in the whole brain. We identified 44 differentially expressed miRNAs (fold change cutoff of ≥ 1.9, *P*-value < 0.05), of which 27 were up-regulated and 17 were down-regulated in UNC0642 treatment (**Figure 1A**). The top 10 up- and down-regulated miRNAs are shown in **Figure 1B**. Then, we validated the increase in the expression of *mmu-miR-1298-5p* (*P* = 0.0061) and the *mmu-miR-669c-5p* (*P* = 0.0717) and the reduction of the *mmu-miR-677-5p* (*P* = 0.0211) and *mmu-miR-128-3p* (*P* = 0.0213) by qRT-PCR (**Figure 1F–I**). These results suggest that UNC0642 treatment induces an alteration in miRNA expression levels.

To determine co-regulation between miRNAs and mRNAs we used the miRTarVis tool (Jung et al., 2015). To determine alterations in mRNA expression, we used our previously reported RNA sequencing (GSE189249) in SAMP8 control and SAMP8-treated mice with UNC0642. We found several nodes with a high number of miRNAs-associated mRNA molecules in our SAMP8 model (**Figure 1C**). On one hand, the up-regulated miRNAs, *mmu-miR-92b-5p*, *mmu-miR-144-3p*, *mmu-miR-34c-5p*, *mmu-miR-204-3p*, *mmu-miR-539-5p*, *mmu-miR-34c-3p*, *mmu-miR-204-5p*, *mmu-miR-208b-3p*, *mmu-miR-148a-5p*, *mmu-miR-34b-5p*, *mmu-miR-448-3p*, and *mmu-miR-187-5p* are associated with the down-regulation of 145 mRNAs (**Figure 1D** and **Additional Tables 5** and **6**). On the other hand, the down-regulated miRNAs, *mmu-miR-34a-3*, *mmu-mir-128-1*, and *mmu-mir-128-2* are associated with the up-regulation of 124 mRNAs (**Figure 1E** and **Additional Tables 5** and **6**) according to miRanda algorithm (Betel et al., 2008). Together, these data show that G9a inhibition with UNC0642 treatment causes a transcriptional dysregulation of miRNAs, which could alter biological processes in the SAMP8 model.

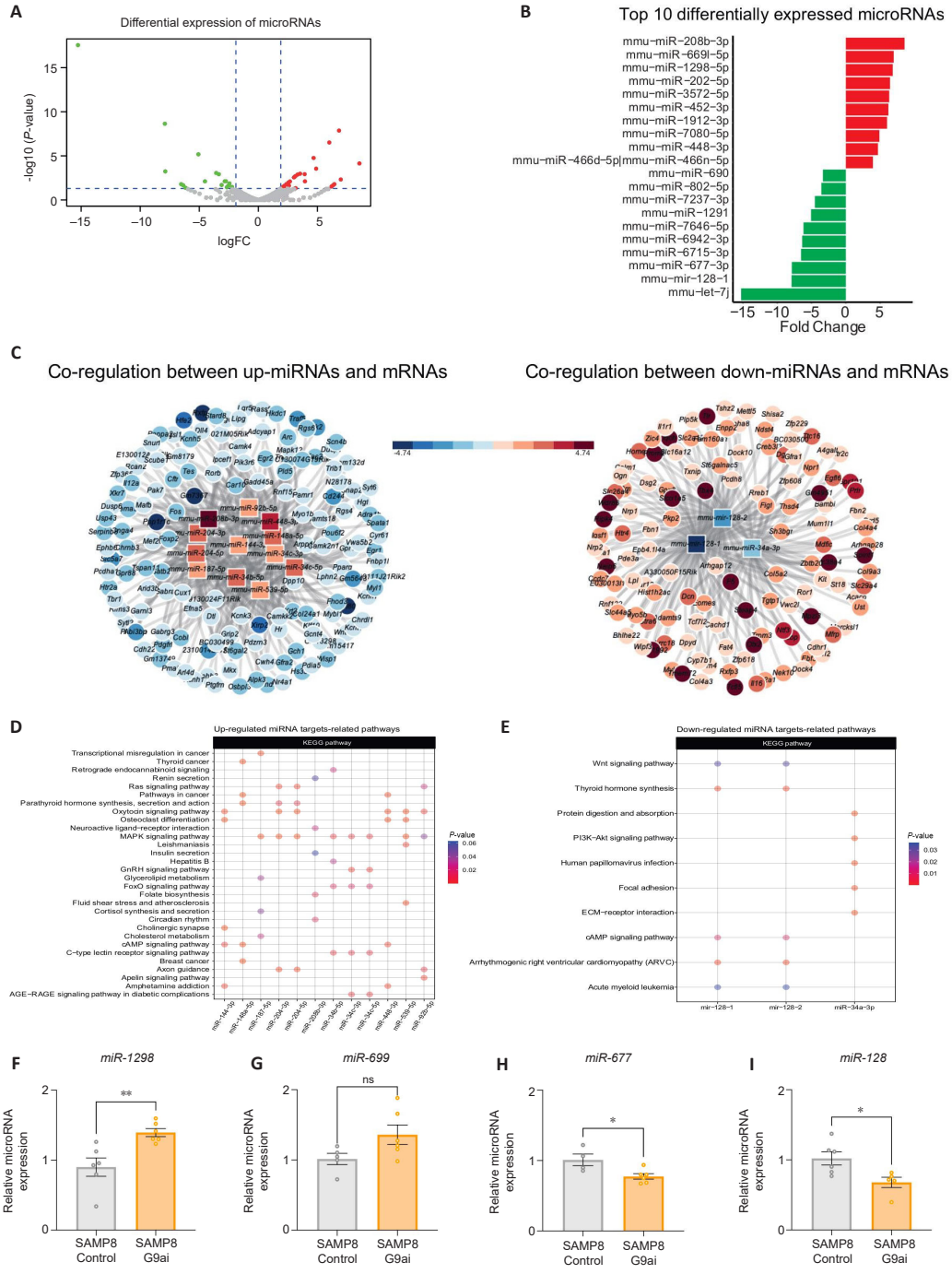


**Figure 1** | **G9a inhibition treatment induces changes in the miRNome.**
(A) Volcano plot showing the differentially expressed microRNAs (miRNAs). (B) Top 10 differentially expressed miRNAs; down-regulated in green and up-regulated in red. (C) A representative network between co-regulation of up-miRNAs and down-mRNAs. (D, E) The dot plots show the top KEGG pathways regulated by target mRNAs in SAMP8 UNC0642. A *P*-value < 0.05 was considered statistically significant. (F–I) miRNA expression levels of *miR-1298*, *miR-669*, *miR-677* and *miR-128*. Values are presented as the mean ± SEM (SAMP8 Control $n = 6$, and SAMP8 G9ai (UNC0642, 5 mg/kg) $n = 6$). $^{*}P < 0.05$, $^{**}P < 0.01$ (Student's *t*-test). ns: Not significant.

### Downregulation of *miR-128-3p* after a G9a inhibition partially explains the modulation of oxidative stress responses and autophagy pathway by targeting *Pparg*

To explore the mechanism underlying the neuroprotective effects of G9ai treatment, the potential mRNAs targeted by *miR-128-3p* were examined for being the second most down-regulated miRNA. MiRNAs require complementary binding with 6 consecutive nucleotides in the 3′ UTR of a target mRNA (Agarwal et al., 2015). Based on Target Scan Human 8.0 (Lewis et al., 2005; Grimson et al., 2007; Friedman et al., 2009; Garcia et al., 2011; Agarwal et al., 2015; McGeary et al., 2019), the 3′-untranslated region (3′-UTR) of PPARG mRNA contains a putative 7-nt *miR-128* target sequence (**Figure 2A**). In accordance, higher *Pparg* gene expression levels were statistically significant in the SAMP8 group treated with G9ai ($P = 0.0001$; **Figure 2B**).

Moreover, gene expression of potential PPARγ target genes was evaluated. First, it was observed that the expression of antioxidant genes, such as superoxide dismutase-1 (*Sod1*), heme oxygenase-1 (*Hmox1*), glutathione peroxidase 1 (*Gpx*),

and aldehyde oxidase-1 (*Aox1*), was significantly up-regulated after treatment with the G9ai ($P$ = 0.0187, 0.0009, 0.0035, 0.0288, respectively; **Figure 2C**). Accordingly, the gene expression levels of cyclooxygenase-2 (*Cox2*) and aldehyde dehydrogenase-2 (*Aldh2*), both pro-oxidant genes, were significantly downregulated in the treated SAMP8 group ($P$ = 0.0476, 0.0090, respectively; **Figure 2D**). Second, we found an increase in the protein levels of FOXO1a in SAMP8 treated with UNC0642 compared with the SAMP8 control group (**Figure 2F** and **H**). Likewise, we observed a statistically significant increase in the p-AMPK/AMPK ratio in the SAMP8-treated group ($P$ = 0.0370; **Figure 2F** and **G**). We also found increased gene expression of deacetylase sirtuin 1 (*Sirt-1*), which regulates the activity of FOXO transcription factors ($P$ = 0.0493; **Figure 2E**), in treated SAMP8 with UNC0642. Then, we assessed the protein levels of antioxidant enzymes. Catalase-3 (CAT3), GPX, and SOD1 were upregulated in the SAMP8 group treated with G9ai compared with the control group ($P$ = 0.02, 0.0203, respectively; **Figure 2I–L**).

To further confirm the antioxidant effects of the G9a inhibition, we treated primary neuron cell cultures with $H_2O_2$ as an oxidative insult. In pathological conditions ($H_2O_2$), we observed a significant increase in cell survival in the group treated with the G9ai *versus* the one treated only with vehicle ($P$ = 0.0003; **Figure 2M**). Then, the antioxidant enzyme glutathione synthetase was upregulated after the pharmacological inhibition of G9a ($P$ = 0.0021; **Figure 2N–O**).

Autophagy can be regulated by the PPARγ/AMPK (Wang et al., 2022). Therefore, we evaluated several autophagy markers. Strikingly, sequestosome-1 (SQSTM1/p62) and Beclin-1 were found upregulated in the SAMP8 treated with the G9ai in comparison with the control ($P$ = 0.0434, 0.0118, respectively; **Figure 3A–C**), suggesting autophagy activation.

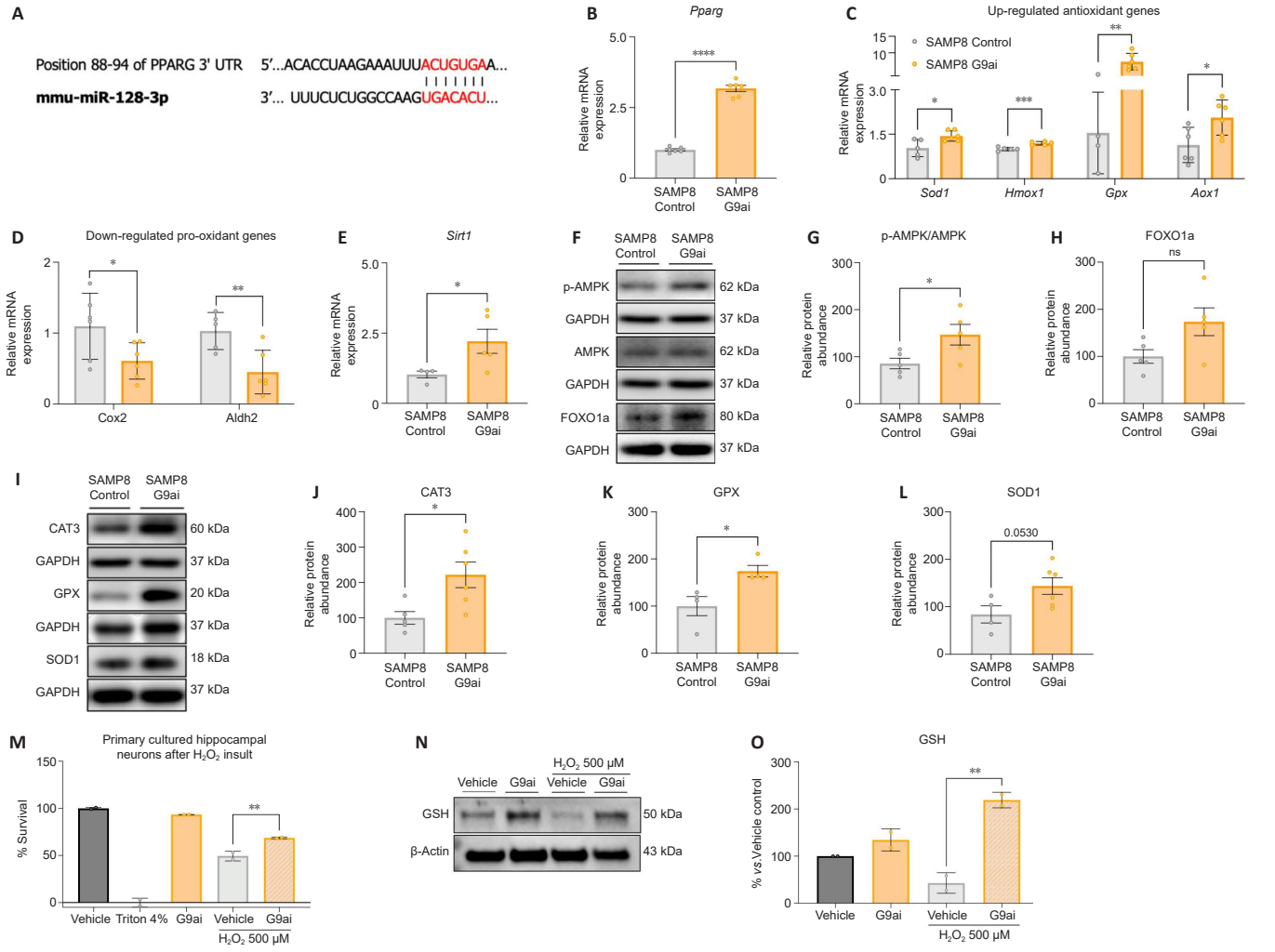


**Figure 2** | **Downregulation of *miR-128* after a G9a inhibition partially explains the modulation of treatment modulates oxidative stress responses by targeting peroxisome-proliferator activator receptor γ (Pparγ).**

(A) Prediction of *miR-128-3p* and PPARG binding sites based on TargetScan. (B) Gene expression levels of peroxisome-proliferator activator receptor γ (*Pparg*). OS pathway: (C) Representation of the expressions of up-regulated antioxidants genes, such as superoxide dismutase-1 (*Sod1*), heme oxygenase-1 (*Hmox1*), glutathione peroxidase 1 (*Gpx*), and aldehyde oxidase-1 (*Aox1*) (grey: SAMP8 Control; orange: SAMP8 G9ai). (D) Representation of the expressions of down-regulated antioxidants genes, such as cyclooxygenase-2 (*Cox2*) and aldehyde dehydrogenase-2 (*Aldh2*) (grey: SAMP8 Control; orange: SAMP8 G9ai). (E) Gene expression of Sirt1. (F–H) Representative western blot bands and quantification of p-AMPK/AMPK ratio, and FOXO1a protein levels. (I–L) Representative western blot bands and quantification of CAT3, GPX, and SOD1 protein levels. Values presented are the mean ± SEM (SAMP8 Control $n$ = 6, and SAMP8 G9ai (UNC0642, 5 mg/kg) $n$ = 6; Student's $t$-test; *$P$ < 0.05, **$P$ < 0.01). (M) Cell survival after $H_2O_2$ insult in primary cultured hippocampal neurons. (N, O) Representative western blot bands and quantification of glutathione synthetase (GSH) protein levels. Values are presented as the mean ± SEM (normal conditions: vehicle group $n$ = 2, Triton 4% group $n$ = 2, G9ai 1 µM $n$ = 2; oxidative stress ($H_2O_2$): vehicle group $n$ = 2, G9ai 1 µM $n$ = 2). **$P$ < 0.01 (one-way analysis of variance followed by Tukey's *post hoc* analysis). ns: Not significant; SAMP8: senescence-accelerated mouse-prone 8.

### Upregulation of PPARγ by G9ai enhances the expression of genes involved in DNA damage response and apoptosis

The growth arrest and DNA damage 45 alpha (GADD45α) plays an important role in DNA repair (Smith et al., 2000), cell cycle (Vairapandi et al., 2002), apoptosis (Tront et al., 2006), angiogenesis, senescence (Tront et al., 2006), and DNA demethylation (Lee et al., 2012) by recruiting demethylation proteins to CpG island promoters (Arab et al., 2019). Consistent with this, we observed an increase in both *Gadd45a* gene expression and protein levels of GADD45α after the pharmacological inhibition of G9a in SAMP8 mice ($P$ = 0.0119, 0.0408, respectively; **Figure 3D–F** and **Additional Table 6**). As we mentioned before, GADD45α plays an important role in apoptosis (Hildesheim et al., 2002; Tront et al., 2006; Salvador et al., 2013; Kleinsimon et al., 2018). Accordingly, three well-established apoptotic markers, B-cell lymphoma 2 (BCL-2), Bcl-2 Associated X-protein (BAX), and Caspase-3 (CASP3), were significantly upregulated in the treated SAMP8 group compared with the control group ($P$ = 0.042, 0.0223, 0.0964, respectively; **Figure 3G–J**).

### PPARγ/GADD45α contributes to the enhancement of synaptic plasticity and neurogenesis after G9a inhibition

Lack of *Gadd45a* promotes alterations in hippocampal memory and long-term potentiation, a phenotype accompanied by reduced levels of memory-related mRNA (Aparisi Rey et al., 2019). Then, we evaluated gene expression levels of immediate early genes (IEGs) after G9ai pharmacological treatment in SAMP8 mice, since they have a relevant role in the regulation of neuronal activity, synaptic plasticity, and neurogenesis (Minatohara et al., 2016; Duclot and Kabbaj, 2017; Kim et al., 2018; Mahringer et al., 2019; Meenakshi et al., 2021). Early growth response 1 (*Egr1*), activity regulated cytoskeleton associated protein (*Arc*), and *Dnmt3a* gene expression levels were found significantly increased in the treated SAMP8 group in comparison with the control SAMP8 group ($P$ = 0.0231, 0.0013, 0.0428, respectively; **Figure 4A**). However, no statistical differences were observed in *Egr2* gene expression levels ($P$ = 0.4063; **Figure 4A**). Synaptic plasticity-related gene expression, such as VGF nerve growth factor inducible (*Vgf*) and transforming growth factor (*Tgf*) were found upregulated after G9ai pharmacological treatment in SAMP8, although the increase was only statistically significant for *Vgf* ($P$ = 0.0007; **Figure 4B**). Likewise, the gene expression of the neurotrophin receptors, *TrkA* and *TrkB*, were upregulated in the SAMP8 treated group ($P$ = 0.001, 0.0337, respectively; **Figure 4B**). Then, we quantified the levels of well-established synaptic plasticity proteins. In the case of postsynaptic density protein 95 (PSD95), we observed significantly increased levels in the SAMP8 mice treated with a G9ai compared with the control group ($P$ = 0.0407; **Figure 4C** and **D**). In contrast, in the case of PSD93 and synapsin IIa (SYN IIa), a positive tendency was observed after pharmacological treatment (**Figure 4C**, **E**, and **F**). In terms of neurogenesis markers, doublecortin (*Dcx*) gene expression levels were increased in the SAMP8-treated group compared with the control groups ($P$ = 0.0001); however, no differences were observed in SRY-Box transcription factor 2 (*Sox2*) gene expression levels between both experimental groups (**Figure 4G** and **H**). Finally, protein levels of neuronal nuclei (NeuN) were increased in the SAMP8 treated with G9ai *versus* the Control SAMP8 group ($P$ = 0.0165; **Figure 4I** and **J**).

## Discussion

In this study, we have identified and explored an unknown molecular pathway based on PPARγ/GADD45α transcriptional repression controlled by G9a which also modulates miRNAs. Several studies suggest that G9a is a contributing factor to neuroinflammation and is upregulated in AD patients (Zheng et al., 2019; Bellver-Sanchis et al., 2023). In addition, a recent study stated that G9a is necessary to produce pro-inflammatory cytokines and reactive oxygen species, which are associated with OS (Mourits et al., 2021). It has been

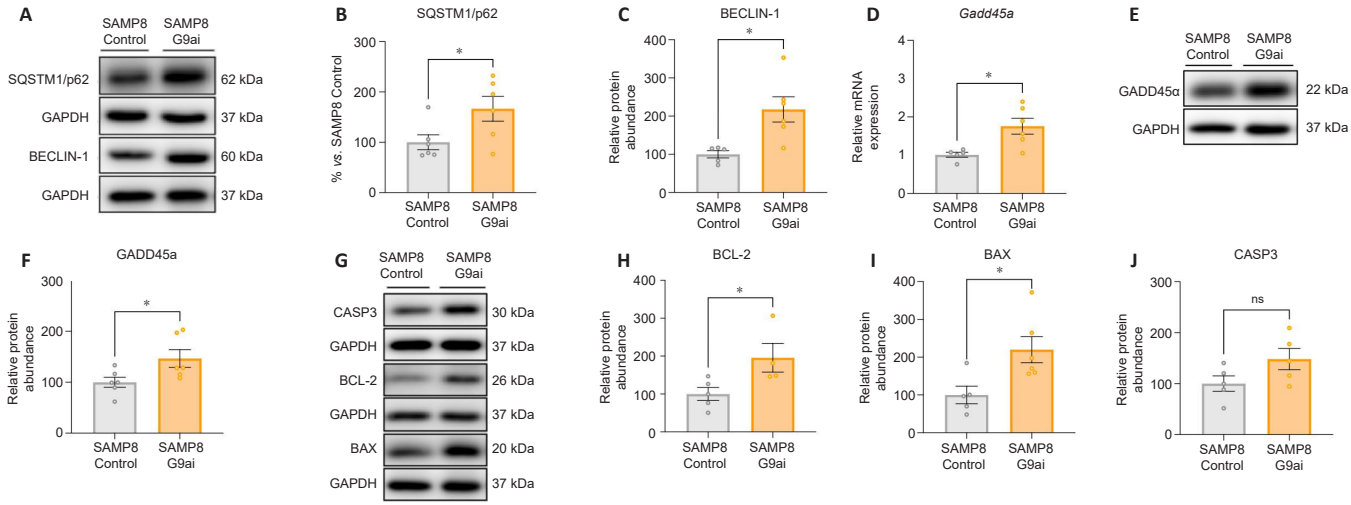


**Figure 3** | **Upregulation of peroxisome-proliferator activator receptor γ (PPARγ) by G9ai enhances the expression of genes involved in DNA damage responses, apoptosis, and autophagy.**

Autophagy pathway: (A–C) Representative western blot bands and quantification of sequestosome-1 (SQSTM1/p62) and BECLIN-1. (D) Gene expression levels of growth arrest and DNA damage 45 alpha (*Gadd45a*). (E, F) Representative western blot bands and quantification of GADD45α. Apoptosis pathway: (G–J) Representative western blot bands and quantification of B-cell lymphoma 2 (BCL-2), Bcl-2 Associated X-protein (BAX), and Caspase-3 (CASP3). Values are presented as the mean ± SEM (SAMP8 Control $n$ = 6, and SAMP8 G9ai (UNC0642, 5 mg/kg) $n$ = 6). *$P$ < 0.05 (Student's $t$-test). ns: Not significant; SAMP8: senescence-accelerated mouse-prone 8.

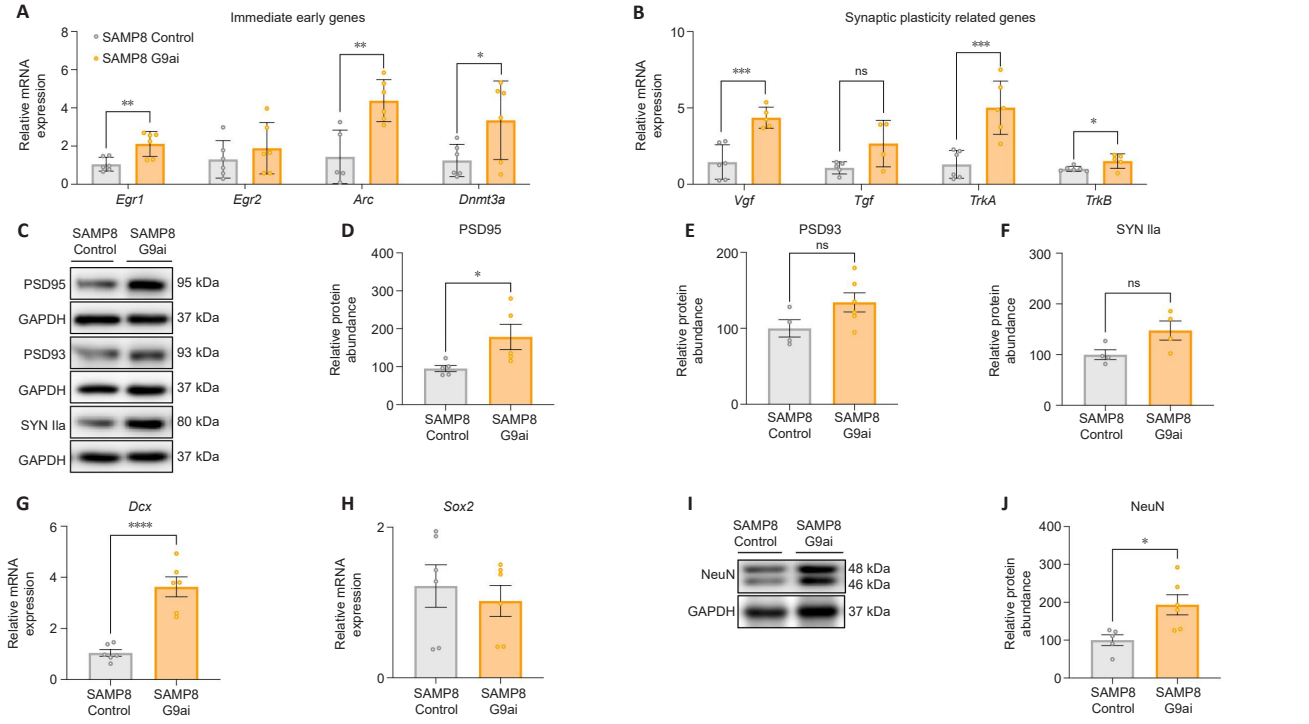


**Figure 4** | **PPARγ/GADD45α might contribute to the enhancement of synaptic plasticity and neurogenesis after G9a inhibition.**
(A) Expression of immediate early genes, *Egr1*, *Egr2*, *Arc*, and DNA methyltransferase (*Dnmt3a*) (grey: SAMP8 Control; Orange: SAMP8 G9ai). (B) Expression of synaptic plasticity-related genes, such as *Vgf*, *Tgf*, *TrkA*, and TrkB (grey: SAMP8 control; orange: SAMP8 G9ai). (C–F) Synaptic plasticity pathway: representative western blot bands and quantification of PSD95, PSD93, and SYN IIa protein levels. (G, H) Gene expression of *Dcx* and *Sox2*. (I, J) Representative western blot bands and quantification of NeuN protein levels. Values are presented as the mean ± SEM (SAMP8 control $n = 6$, and SAMP8 G9ai (UNC0642, 5 mg/kg) $n = 6$). $^*P < 0.05$, $^{**}P < 0.01$, $^{***}P < 0.001$ (Student's *t*-test). Arc: Activity regulated cytoskeleton associated protein; Dcx: doublecortin; Dnmt3a: DNA methyltransferase; Egr: early growth response 1; G9ai: G9a inhibitor; GADD45α: growth arrest and DNA damage 45 alpha; NeuN: neuronal nuclei; PPARγ: peroxisome-proliferator activator receptor gamma; SAMP8: senescence-accelerated mouse-prone 8; Tgf: transforming growth factor; Vgf: VGF nerve growth factor inducible; ns: not significant; Sox2: SRY-Box transcription factor 2.

suggested that G9a is also necessary for the maintenance of epigenetic marks since it can promote or repress gene expression, and thereby affects the expression of several miRNAs (Shankar et al., 2013). Thus, there is evidence of the crosstalk between G9a, miRNAs, OS, and neuroinflammation and its contribution to the pathogenesis of AD.

Specific miRNAs participate in the initiation and progression of neurodegenerative diseases, including AD (Kumar and Reddy, 2020). Indeed, several miRNAs play a role in the control of key components of neuronal functions such as learning and memory formation (Saab and Mansuy, 2014). Furthermore, as aforementioned, miRNAs regulate gene expression at the post-transcriptional level (Gurtan and Sharp, 2013). At first, by overlaying transcriptomic analyses, we identified several miRNAs (*miR-1298*, *miR-669*, *miR-677*, and *miR-128*) that were modified. The KEGG enrichment analysis revealed the association of G9a with cholinergic synapse, axon guidance, and cAMP signaling pathway, among others. But what is more noteworthy is that KEGG enrichment analysis showed that G9ai treatment modulates the MAPK and FOXO signaling pathways, which is further confirmed throughout the work. An example of one of the modulated miRNAs was *miR-1298*, which is downregulated in different pathological conditions and is associated with hypermethylation of its upstream DNA CpG sites (Hu et al., 2015). Accordingly, our results showed a downregulation of *miR-1298* in SAMP8 mice, which was reverted after G9ai, indicating a reduction in DNA methylation levels, allowing the upregulation of this miRNA and thus, modifying the gene transcription of different important neuroprotective genes. We also found an upregulation in *miR-669* after G9a inhibition with UNC0642 in SAMP8 mice. These results are in agreement with recent work from Kolosowska et al. (2020), which showed that the upregulation of *miR-669c-3p* promotes neuroprotective effects in a mouse model of ischemic stroke through induction of the expression of anti-inflammatory microglial markers and PPARγ. The latter is the one we have focused on in this study. Moreover, we found downregulation in *miR-677* and *miR-128* after G9a inhibition. *miR-677* has a role in protein synthesis directly associated with neurodegenerative disease, including AD, such as protein related to neuroactive ligand-receptor, autophagy, and Wnt signaling pathway as we found in SAMP8 after G9ai. Last but not least, *miR-128* is involved in the development of the nervous system as well as the regulation of neuronal plasticity, neuronal death, and cognitive impairment (Hu et al., 2015; Kolosowska et al., 2020). Importantly, recently published research has shown that *miR-128* is increased in the hippocampus of AD human brains (Siedlecki-Wullich et al., 2021). More importantly, *miR-128* downregulation improved cognitive deficits and reduced A pathology in 3×Tg-AD mice (Liu et al., 2019). Furthermore, this improvement in cognition was associated with increased levels of PPARγ. PPARγ is targeted by *miR-128* (Liu et al., 2019). In our case, we found reduced levels of *miR-128* in SAMP8-treated mice with UNC0642, which were correlated with better cognitive performance, as we demonstrated in our previously published manuscript (Bellver-Sanchis et al., 2023), suggesting the regulation of *miR-128* by G9a.

PPARγ is an essential nuclear receptor involved in energy homeostasis and inflammation, which promotes growth interconnection of various pathways, such as the nuclear factor erythroid 2 related factor 2 (NRF2), Wnt/β-catenin, and FOXO (Polvani et al., 2012). Also, several studies have shown that PPARγ is implicated in the OS response, which involves an imbalance between pro-oxidation and anti-oxidation forces that may lead to cell death (Polvani et al., 2012; Vallée and Lecarpentier, 2018; Beheshti et al., 2022). In this regard, we evaluated gene expression related to this molecular pathway. On one hand, the expression of the antioxidant genes evaluated in this work was increased after treatment with G9ai, both for *in vitro* and *in vivo* studies. In the same way, the expression of the pro-oxidant markers was downregulated in the treated SAMP8 mice. It has been observed that PPARγ agonists protected cells from oxidative stress after ischemia by suppressing COX2 expression in a PPARγ-dependent manner (Zhao et al., 2006). On the other hand, one of the more important upregulated signaling pathways in SAMP8-treated mice was FOXO. In accordance with our results, it has been reported that G9a protein levels were elevated and FOXO1 protein levels were decreased in human colon cancer patients (Chae et al., 2019). Hence, to our knowledge, herein we described for the first time the upregulation of the FOXO signaling pathway in the SAMP8 brain after treatment with UNC0642. Interestingly, in the FOXO1-dependent mechanism, AMPK controls the expression of antioxidant enzymes, and therefore this enzyme may have an important role in the maintenance of redox homeostasis (Yun et al., 2014). Accordingly, the increased expression of some of the OS markers evaluated in this work, such as CAT3 or SOD1 (Ding et al., 2007; Yu et al., 2008), is directly related to all PPAR isoforms (Muzio et al., 2021). For example, increased PPARγ has been shown to correlate with increased levels of glutathione synthetase (Ferguson et al., 2009), and HMOX1 (Krönke et al., 2007; Bilban et al., 2009; Ferguson et al., 2009; Polvani et al., 2012). Altogether, these data suggest the activation of molecular pathways that can revert the neuronal damage presented in AD.

In the same manner, the PPARγ/AMPK axis also regulates autophagy (Wang et al., 2022). It is well-known that G9a represses the expression of genes involved in the autophagic process (Artal-Martinez de Narvajas et al., 2013), and its inhibition promotes the activation of the autophagic pathway (Griñán-Ferré et al., 2019). According to this, here we found an induction of autophagy markers (BECLIN-1, SQSTM1/p62, among others) that are associated with the completion of the beneficial effects of the autophagic process after pharmacological inhibition of G9a in SAMP8-treated animals.

PPARγ is found to be correlated with GADD45α protein (Fujiki et al., 2009). GADD45α protein interacts with PPARγ, recruiting demethylation proteins to CpG island promoters, and consequently upregulating its transcriptional activity (Arab et al., 2019), and consequently upregulating transcriptional activity of PPARγ (Fujiki et al., 2009). Indeed, it has been described that *Gadd45* is widely expressed in the mouse brain, including the cerebral cortex and hippocampus, both fundamental regions for memory formation (Matsunaga et al., 2015; Aparisi Rey et al., 2019). Recently, it was shown that *Gadd45a*-deficient mice displayed alterations in hippocampal memory and long-term potentiation, associated with reduced mRNA levels of genes related to memory (Leach et al., 2012). Thus, we evaluated the gene expression levels of IEGs after the pharmacological treatment of SAMP8 mice and found changes in *Egr1* and *Dnmt3a* gene expression, suggesting the improvement in cognition previously demonstrated (Vasilopoulou et al., 2022). Furthermore, these results were accompanied by increased gene expression of neurotrophin receptors, *TrkA* and *TrkB*. Then, we proceed to evaluate the levels of well-established synaptic plasticity proteins. In the case of the protein levels of PSD95, PSD93, and SYN IIa, as well as neurogenesis markers, *Dcx* gene expression levels as well as protein levels of NeuN were increased in the SAMP8 treated with G9ai versus the Control SAMP8 group. Those results were consistent with previous published results by us and others, that showed that elevated H3K9me2 and G9a levels are present in the hippocampus of several AD mice models, promoting diminished synaptic transmission, and learning and memory deficits (Griñán-Ferré et al., 2019; Zheng et al., 2019). Those processes were ameliorated by G9a inhibition with UNC0642 or BIX01294 treatment, pointing to the participation in synaptic dysfunction and cognitive decline of G9a. However, the exact mechanisms by which G9a inhibition promotes miRNA changes remain unclear and require further studies.

The main limitation of this study could be to describe in depth the direct modulation of *miR-128*/*Pparg* by pharmacological inhibition of G9a. Further studies with gene editing or also using a pharmacological approach would be helpful to confirm this. These experiments could provide more robustness to our results, confirming the direct link between G9a and *miR-128*/*Pparg*. However, it has been noted that all the evidence already cited throughout the manuscript agrees with our findings, as well as we report the changes in the miRNome profile after pharmacological treatment of G9a in a well-established AD mice model, the SAMP8.

In conclusion, this study demonstrates that G9a inhibition with UNC0642 improves the gene expression profile of mRNAs and miRNAs in the SAMP8 mouse model. The differentially expressed miRNAs after UNC0642 treatment promote the activation of the PPARγ/GADD45α axis, leading to changes in crucial molecular pathways associated with age-related cognitive decline. Therefore, these results suggest that G9a and miRNAs are promising diagnostic biomarkers and therapeutic targets for neurodegenerative diseases such as AD.

**Author contributions:** *CGF conceived the study. ABS, CGF, PAAL, IT, MRV, and DVG performed the experiments. ABS, CGF, AG, PAAL, IT, and CP designed the experiments and analyzed the data. ABS, DB, LL, GC, AG, MP, and CGF wrote the manuscript. All authors read and approved the final manuscript.*
**Conflicts of interest:** *None of the authors has any disclosures to declare.*
**Author statement:** *This paper has been partially posted as a preprint on Research Square with doi: https://doi.org/10.21203/rs.3.rs-1228952/v1, which is available from: https://assets.researchsquare.com/files/rs-1228952/v1_covered.pdf?c=1641408565.*
**Data availability statement:** *All relevant data are within the paper and its Additional files.*

**Additional files:**
***Additional Table 1:*** *Reagents and kits used in this study.*
***Additional Table 2:*** *TaqMan probes used in this study.*
***Additional Table 3:*** *SYBR Green primers analyzed in this study.*
***Additional Table 4:*** *Antibodies used in western blot assay in this study.*
***Additional Table 5:*** *Differentially expressed miRNAs.*
***Additional Table 6:*** *miRNAs targets.*

## References

Agarwal V, Bell GW, Nam JW, Bartel DP (2015) Predicting effective microRNA target sites in mammalian mRNAs. Elife 4:e05005.

Aparisi Rey A, Karaulanov E, Sharopov S, Arab K, Schäfer A, Gierl M, Guggenhuber S, Brandes C, Pennella L, Gruhn WH, Jelinek R, Maul C, Conrad A, Kilb W, Luhmann HJ, Niehrs C, Lutz B (2019) Gadd45α modulates aversive learning through post-transcriptional regulation of memory-related mRNAs. EMBO Rep 20:e46022.

Arab K, Karaulanov E, Musheev M, Trnka P, Schäfer A, Grummt I, Niehrs C(2019) GADD45A binds R-loops and recruits TET1 to CpG island promoters. Nat Genet 51:217-223.

Artal-Martinez de Narvajas A, Gomez TS, Zhang JS, Mann AO, Taoda Y, Gorman JA, Herreros-Villanueva M, Gress TM, Ellenrieder V, Bujanda L, Kim DH, Kozikowski AP, Koenig A, Billadeau DD (2013) Epigenetic regulation of autophagy by the methyltransferase G9a. Mol Cell Biol 33:3983-3993.

Beheshti F, Gholami M, Ghane Z, Nazari SE, Salari M, Shabab S, Hosseini M (2022) PPARγ activation improved learning and memory and attenuated oxidative stress in the hippocampus and cortex of aged rats. Physiol Rep 10:e15538.

Bellver-Sanchis A, Geng Q, Navarro G, Ávila-López PA, Companys-Alemany J, Marsal-García L, Larramona-Arcas R, Miró L, Perez-Bosque A, Ortuño-Sahagún D, Banerjee DR, Choudhary BS, Soriano FX, Poulard C, Pallàs M, Du HN, Griñán-Ferré C (2023) G9a inhibition promotes neuroprotection through GMFB regulation in Alzheimer's disease. Aging Dis doi: 10.14336/AD.2023.0424-2

Betel D, Wilson M, Gabow A, Marks DS, Sander C (2008) The microRNA.org resource: targets and expression. Nucleic Acids Res 36:D149-153.

Bilban M, Haslinger P, Prast J, Klinglmüller F, Woelfel T, Haider S, Sachs A, Otterbein LE, Desoye G, Hiden U, Wagner O, Knöfler M (2009) Identification of novel trophoblast invasion-related genes: heme oxygenase-1 controls motility via peroxisome proliferator-activated receptor gamma. Endocrinology 150:1000-1013.

Butterfield DA, Poon HF (2005) The senescence-accelerated prone mouse (SAMP8): a model of age-related cognitive decline with relevance to alterations of the gene expression and protein abnormalities in Alzheimer's disease. Exp Gerontol 40:774-783.

Chae YC, Kim JY, Park JW, Kim KB, Oh H, Lee KH, Seo SB (2019) FOXO1 degradation via G9a-mediated methylation promotes cell proliferation in colon cancer. Nucleic Acids Res 47:1692-1705.

Chen EY, Tan CM, Kou Y, Duan Q, Wang Z, Meirelles GV, Clark NR, Ma'ayan A (2013) Enrichr: interactive and collaborative HTML5 gene list enrichment analysis tool. BMC Bioinformatics 14:128.

Cho YW, Hong S, Jin Q, Wang L, Lee JE, Gavrilova O, Ge K (2009) Histone methylation regulator PTIP is required for PPARgamma and C/EBPalpha expression and adipogenesis. Cell Metab 10:27-39.

Cosín-Tomás M, Álvarez-López MJ, Companys-Alemany J, Kaliman P, González-Castillo C, Ortuño-Sahagún D, Pallàs M, Griñán-Ferré C (2018) Temporal integrative analysis of mRNA and microRNAs expression profiles and epigenetic alterations in female SAMP8, a model of age-related cognitive decline. Front Genet 9:596.

Ding G, Fu M, Qin Q, Lewis W, Kim HW, Fukai T, Bacanamwo M, Chen YE, Schneider MD, Mangelsdorf DJ, Evans RM, Yang Q (2007) Cardiac peroxisome proliferator-activated receptor gamma is essential in protecting cardiomyocytes from oxidative damage. Cardiovasc Res 76:269-279.

Duclot F, Kabbaj M (2017) The role of early growth response 1 (EGR1) in brain plasticity and neuropsychiatric disorders. Front Behav Neurosci 11:35.

Eid A, Mhatre I, Richardson JR (2019) Gene-environment interactions in Alzheimer's disease: A potential path to precision medicine. Pharmacol Ther 199:173-187.

Ferguson HE, Thatcher TH, Olsen KC, Garcia-Bates TM, Baglole CJ, Kottmann RM, Strong ER, Phipps RP, Sime PJ (2009) Peroxisome proliferator-activated receptor-gamma ligands induce heme oxygenase-1 in lung fibroblasts by a PPARgamma-independent, glutathione-dependent mechanism. Am J Physiol Lung Cell Mol Physiol 297:L912-919.

Friedman RC, Farh KK, Burge CB, Bartel DP (2009) Most mammalian mRNAs are conserved targets of microRNAs. Genome Res 19:92-105.

Fujiki K, Kano F, Shiota K, Murata M (2009) Expression of the peroxisome proliferator activated receptor gamma gene is repressed by DNA methylation in visceral adipose tissue of mouse models of diabetes. BMC Biol 7:38.

Garcia DM, Baek D, Shin C, Bell GW, Grimson A, Bartel DP (2011) Weak seed-pairing stability and high target-site abundance decrease the proficiency of lsy-6 and other microRNAs. Nat Struct Mol Biol 18:1139-1146.

Ge C, Cawthorn WP, Li Y, Zhao G, Macdougald OA, Franceschi RT (2016) Reciprocal control of osteogenic and adipogenic differentiation by ERK/MAP kinase phosphorylation of Runx2 and PPARγ transcription factors. J Cell Physiol 231:587-596.

Grimson A, Farh KK, Johnston WK, Garrett-Engele P, Lim LP, Bartel DP (2007) MicroRNA targeting specificity in mammals: determinants beyond seed pairing. Mol Cell 27:91-105.

Griñán-Ferré C, Corpas R, Puigoriol-Illamola D, Palomera-Ávalos V, Sanfeliu C, Pallàs M (2018) Understanding epigenetics in the neurodegeneration of Alzheimer's disease: SAMP8 mouse model. J Alzheimers Dis 62:943-963.

Griñán-Ferré C, Marsal-García L, Bellver-Sanchis A, Kondengaden SM, Turga RC, Vázquez S, Pallàs M (2019) Pharmacological inhibition of G9a/GLP restores cognition and reduces oxidative stress, neuroinflammation and β-Amyloid plaques in an early-onset Alzheimer's disease mouse model. Aging (Albany NY) 11:11591-11608.

Gupta-Agarwal S, Franklin AV, Deramus T, Wheelock M, Davis RL, McMahon LL, Lubin FD (2012) G9a/GLP histone lysine dimethyltransferase complex activity in the hippocampus and the entorhinal cortex is required for gene activation and silencing during memory consolidation. J Neurosci 32:5440-5453.

Gurtan AM, Sharp PA (2013) The role of miRNAs in regulating gene expression networks. J Mol Biol 425:3582-3600.

Ha M, Kim VN (2014) Regulation of microRNA biogenesis. Nat Rev Mol Cell Biol 15:509-524.

Harman MF, Martín MG (2020) Epigenetic mechanisms related to cognitive decline during aging. J Neurosci Res 98:234-246.

Hildesheim J, Bulavin DV, Anver MR, Alvord WG, Hollander MC, Vardanian L, Fornace AJ Jr (2002) Gadd45a protects against UV irradiation-induced skin tumors, and promotes apoptosis and stress signaling via MAPK and p53. Cancer Res 62:7305-7315.

Houseknecht KL, Cole BM, Steele PJ (2002) Peroxisome proliferator-activated receptor gamma (PPARgamma) and its ligands: a review. Domest Anim Endocrinol 22:1-23.

Hu W, Wang M, Yin H, Yao C, He Q, Yin L, Zhang C, Li W, Chang G, Wang S (2015) MicroRNA-1298 is regulated by DNA methylation and affects vascular smooth muscle cell function by targeting connexin 43. Cardiovasc Res 107:534-545.

Ionescu-Tucker A, Cotman CW (2021) Emerging roles of oxidative stress in brain aging and Alzheimer's disease. Neurobiol Aging 107:86-95.

Jung D, Kim B, Freishtat RJ, Giri M, Hoffman E, Seo J (2015) miRTarVis: an interactive visual analysis tool for microRNA-mRNA expression profile data. BMC Proc 9:S2

Kapadia R, Yi JH, Vemuganti R (2008) Mechanisms of anti-inflammatory and neuroprotective actions of PPAR-gamma agonists. Front Biosci 13:1813-1826.

Kim S, Kim H, Um JW (2018) Synapse development organized by neuronal activity-regulated immediate-early genes. Exp Mol Med 50:1-7.

Kleinsimon S, Longmuss E, Rolff J, Jäger S, Eggert A, Delebinski C, Seifert G (2018) GADD45A and CDKN1A are involved in apoptosis and cell cycle modulatory effects of viscumTT with further inactivation of the STAT3 pathway. Sci Rep 8:5750.

Kolosowska N, Gotkiewicz M, Dhungana H, Giudice L, Giugno R, Box D, Huuskonen MT, Korhonen P, Scoyni F, Kanninen KM, Ylä-Herttuala S, Turunen TA, Turunen MP, Koistinaho J, Malm T (2020) Intracerebral overexpression of miR-669c is protective in mouse ischemic stroke model by targeting MyD88 and inducing alternative microglial/macrophage activation. J Neuroinflammation 17:194.

Konovalova J, Gerasymchuk D, Parkkinen I, Chmielarz P, Domanskyi A (2019) Interplay between MicroRNAs and Oxidative Stress in Neurodegenerative Diseases. Int J Mol Sci 20:6055.

Krönke G, Kadl A, Ikonomu E, Blüml S, Fürnkranz A, Sarembock IJ, Bochkov VN, Exner M, Binder BR, Leitinger N (2007) Expression of heme oxygenase-1 in human vascular cells is regulated by peroxisome proliferator-activated receptors. Arterioscler Thromb Vasc Biol 27:1276-1282.

Kuleshov MV, Jones MR, Rouillard AD, Fernandez NF, Duan Q, Wang Z, Koplev S, Jenkins SL, Jagodnik KM, Lachmann A, McDermott MG, Monteiro CD, Gundersen GW, Ma'ayan A (2016) Enrichr: a comprehensive gene set enrichment analysis web server 2016 update. Nucleic Acids Re 44:W90- W97.

Kumar S, Reddy PH (2020) The role of synaptic microRNAs in Alzheimer's disease. Biochim Biophys Acta Mol Basis Dis 1866:165937.

Leach PT, Poplawski SG, Kenney JW, Hoffman B, Liebermann DA, Abel T, Gould TJ (2012) Gadd45b knockout mice exhibit selective deficits in hippocampus-dependent long-term memory. Learn Mem 19:319-324.

Lee B, Morano A, Porcellini A, Muller MT (2012) GADD45α inhibition of DNMT1 dependent DNA methylation during homology directed DNA repair. Nucleic Acids Res 40:2481-2493.

Leng F, Edison P (2021) Neuroinflammation and microglial activation in Alzheimer disease: where do we go from here? Nat Rev Neurol 17:157-172.

Lewis BP, Burge CB, Bartel DP (2005) Conserved seed pairing, often flanked by adenosines, indicates that thousands of human genes are microRNA targets. Cell 120:15-20.

Liang Y, Wang L (2021) Inflamma-microRNAs in Alzheimer's disease: from disease pathogenesis to therapeutic potentials. Front Cell Neurosci 15:785433.

Liu B, Liu J, Shi JS (2020) SAMP8 mice as a model of age-related cognition decline with underlying mechanisms in Alzheimer's disease. J Alzheimers Dis 75:385-395.

Liu J, Wang H, Zuo Y, Farmer SR (2006) Functional interaction between peroxisome proliferator-activated receptor gamma and beta-catenin. Mol Cell Biol 26:5827-5837.

Liu Y, Zhang Y, Liu P, Bai H, Li X, Xiao J, Yuan Q, Geng S, Yin H, Zhang H, Wang Z, Li J, Wang S, Wang Y (2019) MicroRNA-128 knockout inhibits the development of Alzheimer's disease by targeting PPARγ in mouse models. Eur J Pharmacol 843:134-144.

Mahringer D, Petersen AV, Fiser A, Okuno H, Bito H, Perrier JF, Keller GB (2019) Expression of c-Fos and Arc in hippocampal region CA1 marks neurons that exhibit learning-related activity changes. BioRxiv doi: https://doi.org/10.1101/644526.

Matsunaga E, Nambu S, Oka M, Iriki A (2015) Comparative analysis of developmentally regulated expressions of Gadd45a, Gadd45b, and Gadd45g in the mouse and marmoset cerebral cortex. Neuroscience 284:566-580.

McGeary SE, Lin KS, Shi CY, Pham TM, Bisaria N, Kelley GM, Bartel DP (2019) The biochemical basis of microRNA targeting efficacy. Science 366:eaav1741.

Meenakshi P, Kumar S, Balaji J (2021) In vivo imaging of immediate early gene expression dynamics segregates neuronal ensemble of memories of dual events. Mol Brain 14:102.

Minatohara K, Akiyoshi M, Okuno H (2016) Role of immediate-early genes in synaptic plasticity and neuronal ensembles underlying the memory trace. Front Mol Neurosci 8:78.

Mourits VP, van Puffelen JH, Novakovic B, Bruno M, Ferreira AV, Arts RJ, Groh L, Crișan TO, Zwaag J, Jentho E, Kox M, Pickkers P, van de Veerdonk FL, Weis S, Oosterwijk E, Vermeulen SH, Netea MG, Joosten LA (2021) Lysine methyltransferase G9a is an important modulator of trained immunity. Clin Transl Immunology 10:e1253.

Muzio G, Barrera G, Pizzimenti S (2021) Peroxisome proliferator-activated receptors (PPARs) and oxidative stress in physiological conditions and in cancer. Antioxidants (Basel) 10:1734.

Nagaraj S, Zoltowska KM, Laskowska-Kaszub K, Wojda U (2019) microRNA diagnostic panel for Alzheimer's disease and epigenetic trade-off between neurodegeneration and cancer. Ageing Res Rev 49:125-143

Park J, Lee K, Kim K, Yi SJ (2022) The role of histone modifications: from neurodevelopment to neurodiseases. Signal Transduct Target Ther 7:217.

Polvani S, Tarocchi M, Galli A (2012) PPARγ and oxidative stress: Con(β) catenating NRF2 and FOXO. PPAR Res 2012:641087.

Rothammer N, Woo MS, Bauer S, Binkle-Ladisch L, Di Liberto G, Egervari K, Wagner I, Haferkamp U, Pless O, Merkler D, Engler JB, Friese MA (2022) G9a dictates neuronal vulnerability to inflammatory stress via transcriptional control of ferroptosis. Sci Adv 8:eabm5500.

Saab BJ, Mansuy IM (2014) Neuroepigenetics of memory formation and impairment: the role of microRNAs. Neuropharmacology 80:61-69.

Salvador JM, Brown-Clay JD, Fornace AJ Jr (2013) Gadd45 in stress signaling, cell cycle control, and apoptosis. Adv Exp Med Biol 793:1-19.

Shankar SR, Bahirvani AG, Rao VK, Bharathy N, Ow JR, Taneja R (2013) G9a, a multipotent regulator of gene expression. Epigenetics 8:16-22.

Shukla S, Tekwani BL (2020) Histone deacetylases inhibitors in neurodegenerative diseases, neuroprotection and neuronal differentiation. Front Pharmacol 11:537.

Siedlecki-Wullich D, Català-Solsona J, Fábregas C, Hernández I, Clarimon J, Lleó A, Boada M, Saura CA, Rodríguez-Álvarez J, Miñano-Molina AJ (2019) Altered microRNAs related to synaptic function as potential plasma biomarkers for Alzheimer's disease. Alzheimers Res Ther 11:46.

Siedlecki-Wullich D, Miñano-Molina AJ, Rodríguez-Álvarez J (2021) microRNAs as early biomarkers of Alzheimer's disease: A synaptic perspective. Cells 10:113.

Smith ML, Ford JM, Hollander MC, Bortnick RA, Amundson SA, Seo YR, Deng CX, Hanawalt PC, Fornace AJ Jr (2000) p53-mediated DNA repair responses to UV radiation: studies of mouse cells lacking p53, p21, and/or gadd45 genes. Mol Cell Biol 20:3705-3714.

Subramanian A, Tamayo P, Mootha VK, Mukherjee S, Ebert BL, Gillette MA, Paulovich A, Pomeroy SL, Golub TR, Lander ES, Mesirov JP (2005) Gene set enrichment analysis: a knowledge-based approach for interpreting genome-wide expression profiles. Proc Natl Acad Sci U S A 102:15545-15550.

Tecalco-Cruz AC, Ramírez-Jarquín JO, Alvarez-Sánchez ME, Zepeda-Cervantes J (2020) Epigenetic basis of Alzheimer disease. World J Biol Chem 11:62-75.

Tront JS, Hoffman B, Liebermann DA (2006) Gadd45a suppresses Ras-driven mammary tumorigenesis by activation of c-Jun NH2-terminal kinase and p38 stress signaling resulting in apoptosis and senescence. Cancer Res 66:8448-8454.

Vairapandi M, Balliet AG, Hoffman B, Liebermann DA (2002) GADD45b and GADD45g are cdc2/cyclinB1 kinase inhibitors with a role in S and G2/M cell cycle checkpoints induced by genotoxic stress. J Cell Physiol 192:327-338.

Vallée A, Lecarpentier Y (2018) Crosstalk between peroxisome proliferator-activated receptor gamma and the canonical WNT/β-catenin pathway in chronic inflammation and oxidative stress during carcinogenesis. Front Immunol 9:745.

Vasilopoulou F, Bellver-Sanchis A, Companys-Alemany J, Jarne-Ferrer J, Irisarri A, Palomera-Ávalos V, Gonzalez-Castillo C, Ortuño-Sahagún D, Sanfeliu C, Pallàs M, Griñán-Ferré C (2022) Cognitive decline and BPSD are concomitant with autophagic and synaptic deficits associated with G9a alterations in aged SAMP8 mice. Cells 11:2603.

Wang L, Jin Q, Lee JE, Su IH, Ge K (2010) Histone H3K27 methyltransferase Ezh2 represses Wnt genes to facilitate adipogenesis. Proc Natl Acad Sci U S A 107:7317-7322.

Wang L, Xu S, Lee JE, Baldridge A, Grullon S, Peng W, Ge K (2013) Histone H3K9 methyltransferase G9a represses PPARγ expression and adipogenesis. EMBO J 32:45-59.

Wang M, Qin L, Tang B (2019) MicroRNAs in Alzheimer's disease. Front Genet 10:153.

Wang S, Li H, Yuan M, Fan H, Cai Z (2022) Role of AMPK in autophagy. Front Physiol 13:1015500.

Wei W, Wang ZY, Ma LN, Zhang TT, Cao Y, Li H (2020) MicroRNAs in Alzheimer's disease: function and potential applications as diagnostic biomarkers. Front Mol Neurosci 13:160.

Xie Z, Bailey A, Kuleshov MV, Clarke DJB, Evangelista JE, Jenkins SL, Lachmann A, Wojciechowicz ML, Kropiwnicki E, Jagodnik KM, Jeon M, Ma'ayan A (2021) Gene set knowledge discovery with Enrichr. Curr Protoc 1:e90.

Yonutas HM, Sullivan PG (2013) Targeting PPAR isoforms following CNS injury. Curr Drug Targets 14:733-742

Yu X, Shao XG, Sun H, Li YN, Yang J, Deng YC, Huang YG (2008) Activation of cerebral peroxisome proliferator-activated receptors gamma exerts neuroprotection by inhibiting oxidative stress following pilocarpine-induced status epilepticus. Brain Res 1200:146-158.

Yun H, Park S, Kim MJ, Yang WK, Im DU, Yang KR, Hong J, Choe W, Kang I, Kim SS, Ha J (2014) AMP-activated protein kinase mediates the antioxidant effects of resveratrol through regulation of the transcription factor FoxO1. FEBS J 281:4421-4438.

Zhao Y, Patzer A, Herdegen T, Gohlke P, Culman J (2006) Activation of cerebral peroxisome proliferator-activated receptors gamma promotes neuroprotection by attenuation of neuronal cyclooxygenase-2 overexpression after focal cerebral ischemia in rats. FASEB J 20:1162-1175.

Zheng Y, Liu A, Wang ZJ, Cao Q, Wang W, Lin L, Ma K, Zhang F, Wei J, Matas E, Cheng J, Chen GJ, Wang X, Yan Z (2019) Inhibition of EHMT1/2 rescues synaptic and cognitive functions for Alzheimer's disease. Brain 142:787-807.

*C-Editor: Zhao M; S-Editor: Li CH; L-Editors: Li CH, Song LP; T-Editor: Jia Y*

**Additional Table 1 Reagents and kits used in this study**

| Reagent/kits | Source | Cat# |
|---|---|---|
| UNC0642 | BLDpharm, Shangai, China | BD630326 |
| 2-hydroxypropyl-β-cyclodextrin | Atomole Scientific Co. Ltd., Wuhan, Hubei, China | AT-20762 |
| TRItidy G™ | PannReac AppliChem, Spain, | A4051, 0,200 |
| High Capacity cDNA Reverse Transcription kit | Applied Biosystems, Vilnius, Lithuania | 4368814 |
| Maxima SYBR Green qPCR Master Mix (2X), ROX solution provided | Thermo Scientific, Vilnius, Lithuania | K0253 |
| mirVana miRNA Isolation kit with phenol | Invitrogen, Foster City, CA, USA | AM1560 |
| TaqMan miRNA Reverse Transcription kit | Thermo Fischer Scientific, Waltham, MA, USA, | 4366596 |
| TaqMan™ Universal PCR Master Mix | Applied Biosystems | 4305719 |
| Trypsin-EDTA (0.25%), phenol red | Gibco, Waltham, MA USA | 25200056 |
| DMEM-F12 medium | Gibco | 12400-024 |
| HyClone Standard Fetal Bovine Serum (FBS) | Cytiva, Marlborough, MA, USA | SH30088.03 |
| Poly-D-lysine | Santa Cruz Biotechnology, Dallas, TX, USA | sc-136156 |
| Neurobasal medium | Gibco | 21103049 |
| B27 supplement | Gibco | 17504044 |
| GlutaMAX™ | Gibco | 35050061 |
| Penicillin-Streptomycin | Gibco | 15140-122 |
| LDH assay | Roche, Indianapolis, IN, USA | 4744926001 |
| Triton X-100 | Sigma-Aldrich, St. Louis, MO, USA | 9036-19-5 |

**Additional Table 2 TaqMan probes used in this study**

| Target | Product size (bp) | Cat# |
|---|---|---|
| *mmu-miR-1298* | - | 4427975 |
| *mmu-miR-677* | - | 4440886 |
| *mmu-miR-669* | - | 4440886 |
| *mmu-miR-128* | - | 4440886 |
| *U6 snRNA* | - | 4427975 |

**Additional Table 3 SYBR Green primers analyzed in this study**

| Target | Forward primer (5'-3') | Forward primer (3'-5') |
|---|---|---|
| *Pparg* | CATTCTGGCCCACCAACTTTGG | TGGAGATGCAGGCTCCACTTTG |
| *Sod-1* | CCACACCTTCACTGGTCCAT | CTAGCGAGTTATGGCGACG |
| *Hmox-1* | TGACACCTGAGGTCAAGCAC | GTCTCTGCAGGGGCAGTATC |
| *Gpx* | GTCACGGTTTTGGGCTTTCC | CTGGTGACCGAGTGGAACAA |
| *Aox-1* | CATAGGCGGCCAGGAACATT | TCCTCGTTCCAGAATGCAGC |
| *Cox-2* | TGACCCCCAAGGCTCAAATA | CCCAGGTCCTCGCTTATGATC |
| *Aldh-2* | GCAGGCGTACACAGAAGTGA | TGAGCTTCATCCCCTACCCA |
| *Sirt-1* | AACACACACACAAAATCCAGCA | TGCAACCTGCTCCAAGGTAT |
| *Gadd45a* | CTGCAGAGCAGAAGACCGAA | GGGTCTACGTTGAGCAGCTT |
| *Egr1* | CCACCATGGACAACTACCCC | TCATAGGGTTGTTCGCTCGG |
| *Egr2* | ACAGGCAGGAGAGAGTCAGT | GAAGATGGTCACCGACGAGG |
| *Arc* | GCCCCCAGCAGTGATTCATA | GGAACCCATGTAGGCAGCTT |
| *Dnmt3a* | ACGCCAAAGAAGTGTCTGCT | CTTTGCCCTGCTTTATGGAG |
| *Vgf* | GTCAGACCCATAGCCTCCC | CTCGGACTGAAATCTCGAAGTTC |
| *Tgf* | CAGGGTGAAGGGGAAAACTC | AGTTCGGTCATTCAGTCTCGC |
| *TrkA* | CTCCTTCTCGCCAGTGGAC | TGCCCTCAGTAGGGGAAAGA |
| *TrkB* | CGTCACTTCGCCAGCAGTAG | CTATACGCCAGGCACCACTC |
| *Dcx* | CCAGCAGTCAGCTCTCAACA | GTACAGGTCCTTGTGCCTCC |
| *Sox2* | CCCCGGGCTGCAGGAAT | TGTGCATCTTGGGGTTCTCC |
| *ß-actin* | CAACGAGCGGTTCCGAT | CAACGAGCGGTTCCGAT |

Aldh-2: Aldehyde dehydrogenase; Aox-1: aldehyde oxidase 1; Arc: activity regulated cytoskeleton associated protein; Cox-2: cyclooxygenase 2; Dcx: doublecortin; DNMT3a: DNA methyltransferase 3 alpha; Egr1/2: early growth response 1/2; Gadd45a: growth arrest and DNA damage inducible alpha; Gpx: glutathione peroxidase 1; Hmox-1: heme oxygenase 1; Pparg; peroxisome proliferator activated receptor gamma; Sirt-1: sirtuin 1; Sod-1: superoxide dismutase 1; Sox2: SRY-box transcription factor 2; Tgf: transforming growth factor; TrkA/B: receptor tyrosine kinase A/B; Vgf: VGF nerve growth factor inducible.

**Additional Table 4 Antibodies used in western blot assay in this study**

| Antibody | Host | Source/Cat#/RRID | WB dilution |
|---|---|---|---|
| p-AMPK | Rabbit | Cell Signaling Technology, Danvers, MA, USA/2532/AB_330331 | 1:1000 |
| AMPK | Rabbit | Cell Signaling Technology/2537/AB_659805 | 1:1000 |
| FOXO1a | Rabbit | Cell Signaling Technology/2880/AB_2106495 | 1:1000 |
| Catalase-3 | Rabbit | Cell Signaling Technology/12980/AB_2798079 | 1:1000 |
| GPX | Rabbit | Novus Biological, CO, USA/NBP1-33620/ AB_10004091 | 1:1000 |
| SOD-1 | Sheep | Millipore, Burlington, MA, USA/574597/AB_2255005 | 1:1000 |
| GSH | Rabbit | Abcam, Waltham, MA, USA/ab124811/AB_10973222 | 1:1000 |
| GADD45α | Mouse | Santa Cruz Biotechnology, TX, USA/sc-6850/AB_627653 | 1:500 |
| BCL-2 | Rabbit | Cell Signaling Technology /2870/AB_2290370 | 1:1000 |
| BAX | Rabbit | Cell Signaling Technology/41162/AB_2924730 | 1:1000 |
| Caspase-3 | Rabbit | BD Transduction Laboratories/C31720/AB_2335903 | 1:1000 |
| SQSTM1/p62 | Mouse | Santa Cruz Biotechnology/sc-28359/AB_628279 | 1:500 |
| BECLIN-1 | Rabbit | Cell Signaling Technology/3738/AB_490837 | 1:1000 |
| PSD95 | Rabbit | Abcam/ab18258/AB_444362/NA | 1:1000 |
| PSD93 | Rabbit | GeneTex, Irvine, CA, USA/GTX133250/AB_2886890 | 1:1000 |
| SYN IIa | Rabbit | Dako, Santa Clara, CA, USA /CloneSY38/NA | 1:1000 |
| NeuN | Mouse | Abcam/ab178846/AB_2636859 | 1:1000 |
| Actin | Mouse | Sigma-Aldrich, St. Louis, MO, USA /A-5441/AB_476744 | 1:2500 |
| GAPDH | Mouse | Millipore /MAB374/AB_2107445 | 1:5000 |
| Goat-anti-mouse HRP conjugated | Goat | Biorad, Hercules, CA, USA/170-5047/AB_11125753 | 1:2000 |
| Goat-anti-rabbit HRP conjugated | Goat | Biorad/170-6515/AB_11125142 | 1:2000 |

(p-)AMPK: (phosphorylated-) Adenosine monophosphate-activated protein kinase; BAX: Bcl-2-associated X protein; BCL-2: B-cell lymphoma 2; FOXO1a: forkhead box protein O1; GADD45α: growth arrest and DNA damage inducible alpha; GAPDH: glyceraldehyde-3-phosphate dehydrogenase; GPX: glutathione peroxidase; GSH: glutathione; NA: not available; NeuN: neuronal nuclei; PSD95: postsynaptic density protein 95; SOD-1: superoxyde dismutase 1; SQSTM1/p62: sequestosome 1; SYN IIa: synapsin IIa.

**Additional Table 5 Differentially expressed miRNAs**

| *miRNA* | Log fold change | Log counts per million | *P*-value |
|---|---|---|---|
| *mmu-let-7j* | 15.2687362 | 8.93267811 | 2.7628E-18 |
| *mmu-mir-128-1* | 7.91104045 | 3.86978577 | 2.2849E-09 |
| *mmu-miR-677-3p* | 7.87675113 | -1.3732063 | 0.00057812 |
| *mmu-miR-6715-3p* | 6.53263092 | -2.4946678 | 0.01625387 |
| *mmu-miR-6942-3p* | 6.3646525 | -2.6163294 | 0.02167183 |
| *mmu-miR-7646-5p* | 6.17450633 | -2.7482791 | 0.04072398 |
| *mmu-miR-1291* | 5.07360856 | 3.62047055 | 6.6835E-06 |
| *mmu-miR-7237-3p* | 4.51855472 | -1.6993221 | 0.00775791 |
| *mmu-miR-802-5p* | 3.57005461 | 1.6636214 | 0.00087489 |
| *mmu-miR-690* | 3.34601258 | 3.88165459 | 0.00119641 |
| *mmu-mir-128-2* | 3.10779292 | -1.5528322 | 0.02011138 |
| *mmu-miR-1941-3p* | 2.83854221 | 0.65391609 | 0.00769132 |
| *mmu-miR-1949* | 2.74579341 | 1.68612831 | 0.00764228 |
| *mmu-miR-6929-3p* | 2.66057011 | -1.2558981 | 0.0359578 |
| *mmu-miR-6990-5p* | 2,55822987 | -0,7148019 | 0.0258626 |
| *mmu-miR-6481* | 2.44209236 | 5.26687132 | 0.01343157 |
| *mmu-miR-34a-3p* | 2.22377906 | 0.60988426 | 0.03362583 |
| *mmu-miR-187-5p* | -1.9719857 | 1.9230752 | 0.04796803 |
| *mmu-miR-877-5p* | -2.059489 | 2.24842384 | 0.03820115 |
| *mmu-miR-7a-2-3p* | -2.0595942 | 4.59869511 | 0.03478584 |
| *mmu-miR-539-5p* | -2.1685846 | -0.119102 | 0.04612425 |
| *mmu-miR-1298-3p* | -2.1973564 | 4.7557324 | 0.02516376 |
| *mmu-miR-144-3p* | -2.3682441 | 4.77302249 | 0.01645278 |
| *mmu-miR-92b-5p* | -2.3773874 | 2.70168661 | 0.01740784 |
| *mmu-miR-34b-3p* | -2.5417088 | 4.26862977 | 0.01061103 |
| *mmu-miR-1264-5p* | -2.5936658 | -0.1126349 | 0.02374869 |
| *mmu-miR-34c-3p* | -2.6749442 | 3.25981439 | 0,00797272 |
| *mmu-miR-204-5p* | -3.0145851 | 10.2735647 | 0.00278358 |
| *mmu-miR-1264-3p* | -3.0983169 | 7.65965958 | 0.0022024 |
| *mmu-miR-34c-5p* | -3,1327463 | 6.49555023 | 0.00202504 |
| *mmu-miR-148a-5p* | -3.1595987 | -1.9930737 | 0.04615818 |
| *mmu-miR-34b-5p* | -3.3253556 | 3.62327107 | 0.00131442 |
| *mmu-miR-204-3p* | -3.535278 | 1.80537606 | 0.00105262 |
| *mmu-miR-1912-5p* | -3.9200743 | 0.56866704 | 0.00118626 |
| *mmu-miR-466d-5p\|mmu-miR-466n-5p* | -3.9470228 | -1.3907703 | 0.00775791 |
| *mmu-miR-448-3p* | -4.6805698 | 6.7736446 | 1.7266E-05 |
| *mmu-miR-7080-5p* | -4.8914647 | 0.24451005 | 0.00028447 |
| *mmu-miR-1912-3p* | -6.0065082 | 4.77360594 | 3.0439E-07 |
| *mmu-miR-452-3p* | -6.1996603 | -2.4019807 | 0.02941176 |
| *mmu-miR-3572-5p* | -6.3235545 | -2.312375 | 0.02167183 |

| | | | |
|---|---|---|---|
| *mmu-miR-202-5p* | -6.4376454 | -2.228299 | 0.01625387 |
| *mmu-miR-1298-5p* | -6.833234 | 7.66313366 | 1.3649E-08 |
| *mmu-miR-669l-5p* | -6.9798677 | -1.8103897 | 0.00474308 |
| *mmu-miR-208b-3p* | -8.5571904 | -0.4712288 | 7.244E-05 |

**Additional Table 6 miRNAs targets**

| mmu-miR-34a-3p | mmu-mir-128-1 | mmu-mir-128-2 | mmu-miR-92b-5p | mmu-miR-144-3p | mmu-miR-34c-5p | mmu-miR-204-3p | mmu-miR-539-5p | mmu-miR-34c-3p | mmu-miR-204-5p | mmu-miR-208b-3p | mmu-miR-148a-5p | mmu-miR-34b-5p | mmu-miR-448-3p | mmu-miR-187-5p |
|---|---|---|---|---|---|---|---|---|---|---|---|---|---|---|
| Mdfic | Nrp1 | Nrp1 | Camk2n1 | Myo1b | Myo1b | 9430021M05Rik | Hs3st2 | Myo1b | 9430021M05Rik | Tes | 2310014L17Rik | Myo1b | Myo1b | Lipg |
| Il16 | Slc44a5 | Slc44a5 | Myo1b | Camk4 | 2310014L17Rik | Rcan2 | Tes | 2310014L17Rik | Rcan2 | Gm8179 | Tes | 2310014L17Rik | Tes | Chrnb3 |
| A4galt | Nrp2 | Nrp2 | Gm7367 | Pld5 | Gadd45a | Pla2g4e | Camk4 | Gadd45a | Pla2g4e | Gch1 | Pld5 | Gadd45a | Camk4 | Krt80 |
| Prlr | Mdfic | Mdfic | Egr2 | Garnl3 | Xirp2 | Garnl3 | Pla2g4e | Xirp2 | Garnl3 | Col24a1 | Gadd45a | Xirp2 | Traf5 | 2310014L17Rik |
| Tcfl5 | Car12 | Car12 | 9430021M05Rik | Snurf | N28178 | Gadd45a | Pld5 | N28178 | Gadd45a | Rorb | Cnga4 | N28178 | Pld5 | Mef2c |
| Iqch | Gm11992 | Gm11992 | Camk4 | Kcnh5 | Adamts18 | Xirp2 | Osbpl3 | Adamts18 | Xirp2 | Adcyap1 | Adcyap1 | Adamts18 | Kcnh7 | Gpr88 |
| Tgtp1 | Pde3a | Pde3a | Rassf3 | Gm13298 | Car10 | Ppp1r1c | Garnl3 | Car10 | Ppp1r1c | Car10 | Adamts18 | Car10 | Cnga4 | Satb2 |
| Mfrp | Htr4 | Htr4 | Pld5 | Pappa2 | Cd244 | Ephb6 | Xirp2 | Cd244 | Ephb6 | Bend7 | Ephb3 | Cd244 | Kcnh5 | Mkx |
| Cdhr1 | Epb4.1l4a | Epb4.1l4a | Hfe2 | Adamts18 | Tmem132d | Kcnk3 | Il12a | Tmem132d | Kcnk3 | Chrnb3 | Trib1 | Gabra3 | Car10 | Dusp6 |
| Htr2c | Stra6 | Stra6 | Lphn2 | Car10 | Gabra3 | Dpp10 | Gm13298 | Gabra3 | Dpp10 | Gpr88 | Dll4 | Kcnk3 | Ppp1r1c | Tspan11 |
| Tmem72 | Lrrc18 | Lrrc18 | Adamts18 | Trib1 | Kcnk3 | Gpr88 | Ppp1r1c | Kcnk3 | Gpr88 | Mafb | Mafb | Fhod3 | Serpinb8 | Arpp19 |
| St6galnac5 | Dpyd | Dpyd | Gk2 | Ppp1r1c | Fhod3 | Mafb | Rgs4 | Fhod3 | Mafb | Pdgfrl | Gm15417 | Arid3b | Rgs4 | Nr4a1 |
| Shisa2 | Wdr86 | Wdr86 | Ppp1r1c | Dll4 | Arid3b | Pak7 | Chrnb3 | Arid3b | Pak7 | Lgr5 | Gfra2 | Krt20 | Kcnk3 | |
| Arhgap12 | Gfra1 | Gfra1 | Dpp10 | Chrnb3 | Krt20 | Arid3b | Gabra3 | Krt20 | Arid3b | Dtl | Wnt10a | Grip2 | Dpp10 | |
| Figf | Lbp | Lbp | Mef2c | Tnfrsf11b | Grip2 | Tac2 | Dpp10 | Grip2 | Tac2 | Pcdha12 | Rgs6 | Camkk2 | Usp43 | |
| Col5a2 | A330050F15Rik | A330050F15Rik | Gpr88 | Pdgfrl | Camkk2 | Gabrg3 | Tnfrsf11b | Camkk2 | Gabrg3 | | Ipcef1 | Tspan11 | Krt80 | |
| Adamts9 | St6galnac5 | St6galnac5 | Pak7 | Htr2a | Tspan11 | Krt20 | Dusp1 | Tspan11 | Krt20 | | Arpp19 | Vwa5b2 | Spata1 | |
| Col9a3 | Cyp7b1 | Cyp7b1 | 9130024F11Rik | Pak7 | Vwa5b2 | Camkk2 | Pdgfrl | Vwa5b2 | Camkk2 | | Slc5a7 | Mapk12 | Grip2 | |
| Cachd1 | Slc2a12 | Slc2a12 | Gabrg3 | Pou6f2 | Mapk12 | Rasgef1b | Cdh22 | Mapk12 | Rasgef1b | | Camk2n1 | Gpr153 | Ipcef1 | |
| Ebf3 | Arhgap12 | Arhgap12 | Efna5 | Ipcef1 | Gpr153 | C130074G19Rik | Pou6f2 | Gpr153 | C130074G19Rik | | Cftr | Gm7367 | Arpp19 | |
| Mettl5 | Figf | Figf | Foxp2 | Arpp19 | Egr1 | Satb2 | Gfra2 | Egr1 | Satb2 | | Egr2 | Egr2 | Pcdha12 | |
| Trpm3 | Col5a2 | Col5a2 | Arpp19 | Pdia5 | Gm7367 | Hr | 9930111J21Rik2 | Gm7367 | Hr | | Gm8179 | Gm5643 | Gm7367 | |
| Dcn | Txnip | Txnip | | Slc5a7 | Egr2 | Cux1 | Ipcef1 | Egr2 | Cux1 | | Hgf | Satb2 | Rims3 | |
| Zfp229 | Ndst4 | Ndst4 | | Camk2n1 | Gm5643 | Rorb | Arpp19 | Gm5643 | Rorb | | Hkdc1 | Hr | Gm8179 | |
| Dock4 | Gm4951 | Gm4951 | | Cftr | Satb2 | Pamr1 | Camk2n1 | Satb2 | Pamr1 | | Fos | Alpk3 | Gcnt4 | |
| Tshz2 | Adamts | Adamts | | Arl4d | Hr | Pdzrn3 | Cftr | Hr | Pdzrn3 | | Cux1 | Cux1 | Hgf | |

| | | | | | | | | | | | |
|---|---|---|---|---|---|---|---|---|---|---|---|
| | 9 | 9 | | | | | | | | | |
| Marcksl 1 | Gpx8 | Gpx8 | Gch1 | Alpk3 | Xkr7 | Adra1b | Alpk3 | Xkr7 | Rorb | Rorb | Tbr1 |
| Myh8 | Cachd1 | Cachd1 | Gcnt4 | Cux1 | Mef2c | Scube1 | Cux1 | Mef2c | Lphn2 | Pdzrn3 | Fos |
| Acacb | Trpm3 | Trpm3 | Col24a1 | Pdzrn3 | BC030499 | Col24a1 | Pdzrn3 | BC030499 | Pparg | BC030499 | Rorb |
| Thsd4 | Dcn | Dcn | Satb2 | Arc | St6gal2 | Fos | Arc | St6gal2 | Pamr1 | Cwh43 | Scn4b |
| Fbn2 | Prom2 | Prom2 | Ptgfrn | BC030499 | Cobl | Lphn2 | BC030499 | Cobl | Mybl1 | Klf10 | Pparg |
| Naip6 | F5 | F5 | Fos | Cwh43 | E130012A19Rik | Rnf152 | Cwh43 | E130012A19Rik | Mef2c | Efna5 | Mybl1 |
| Arhgap28 | Wipf3 | Wipf3 | Rorb | Klf10 | Rgsl1 | Pdzrn3 | Klf10 | Rgsl1 | Snap25 | Dtl | Syt6 |
| Creb3l3 | Gria1 | Gria1 | Zfp365 | Efna5 | Abi3bp | Sema3a | Efna5 | Abi3bp | St6gal2 | Foxp2 | Sema3a |
| Pvrl2 | Fam160a1 | Fam160a1 | Pparg | Dtl | Pik3r6 | Kcnh1 | Dtl | Pik3r6 | Cobl | | Mef2c |
| Gpr101 | Epha8 | Epha8 | Pamr1 | Foxp2 | Efna5 | Mef2c | Foxp2 | Efna5 | Wisp1 | | Stard8 |
| Eomes | Bhlhe22 | Bhlhe22 | Rnf152 | | Dtl | Snap25 | | Dtl | 9130024F11Rik | | Myl1 |
| Pcdh8 | Slco1a5 | Slco1a5 | Gm13749 | | Foxp2 | BC030499 | | Foxp2 | Kcnt1 | | Pmaip1 |
| Slc38a4 | Kit | Kit | Stard8 | | | Klf10 | | | | | Rxfp2 |
| Zbtb20 | Rxfp3 | Rxfp3 | Cobl | | | 9130024F11Rik | | | | | Mkx |
| Tcf7l2 | Pkp2 | Pkp2 | 9130024F11Rik | | | Mkx | | | | | Dtl |
| Drd5 | Dsg2 | Dsg2 | Pik3r6 | | | Efna5 | | | | | Sytl2 |
| Col2a1 | Ror1 | Ror1 | Dtl | | | Dtl | | | | | |
| Spint1 | Slc26a4 | Slc26a4 | Fnbp1l | | | Foxp2 | | | | | |
| Dgkk | Thsd4 | Thsd4 | Foxp2 | | | Chrdl1 | | | | | |
| Col4a3 | Hist1h2ac | Hist1h2ac | Cyr61 | | | | | | | | |
| Col4a4 | Npr1 | Npr1 | | | | | | | | | |
| Nek10 | Myo5b | Myo5b | | | | | | | | | |
| Rreb1 | Lpl | Lpl | | | | | | | | | |
| Tbx4 | Enpp2 | Enpp2 | | | | | | | | | |
| Vwc2l | Rnf122 | Rnf122 | | | | | | | | | |
| Ust | St18 | St18 | | | | | | | | | |
| Fat4 | Egfl6 | Egfl6 | | | | | | | | | |
| Ttc16 | Ttr | Ttr | | | | | | | | | |
| Slc29a4 | Golm1 | Golm1 | | | | | | | | | |
| | Pcdh8 | Pcdh8 | | | | | | | | | |
| | BC030500 | BC030500 | | | | | | | | | |
| | Steap4 | Steap4 | | | | | | | | | |
| | Ccdc78 | Ccdc78 | | | | | | | | | |
| | Ntf3 | Ntf3 | | | | | | | | | |
| | Ripk4 | Ripk4 | | | | | | | | | |
| | Slc38a4 | Slc38a4 | | | | | | | | | |

| | |
|---|---|
| *Otx2* | *Otx2* |
| *Zbtb20* | *Zbtb20* |
| *Sh3bgr* | *Sh3bgr* |
| *Zfp618* | *Zfp618* |
| *Tcf7l2* | *Tcf7l2* |
| *Dock10* | *Dock10* |
| *Zic4* | *Zic4* |
| *Rreb1* | *Rreb1* |
| *Homer3* | *Homer3* |
| *Slc16a1 2* | *Slc16a1 2* |
| *E03001 3I19Rik* | *E03001 3I19Rik* |
| *Tbx4* | *Tbx4* |
| *Vwc2l* | *Vwc2l* |
| *Mpzl3* | *Mpzl3* |
| *Igsf1* | *Igsf1* |
| *Lrrn4* | *Lrrn4* |
| *Ogn* | *Ogn* |
| *Mum1l 1* | *Mum1l 1* |
| *Fat4* | *Fat4* |
| *Bambi* | *Bambi* |
| *Il1r1* | *Il1r1* |
| *A2m* | *A2m* |
| *Pip5k1 b* | *Pip5k1 b* |
| *Fbn1* | *Fbn1* |
| *Zfp608* | *Zfp608* |